*Human Molecular Genetics, 2006, Vol. 15, No. 10* **1600–1609**
*doi:10.1093/hmg/ddl081*
*Advance Access published on March 29, 2006*

# WFS1-deficiency increases endoplasmic reticulum stress, impairs cell cycle progression and triggers the apoptotic pathway specifically in pancreatic β-cells

**Takahiro Yamada[1], Hisamitsu Ishihara[1,*], Akira Tamura[1], Rui Takahashi[1], Suguru Yamaguchi[1], Daisuke Takei[1], Ai Tokita[1], Chihiro Satake[1], Fumi Tashiro[3], Hideki Katagiri[2], Hiroyuki Aburatani[4], Jun-ichi Miyazaki[3] and Yoshitomo Oka[1]**

[1]Division of Molecular Metabolism and Diabetes and [2]Division of Advanced Therapeutics for Metabolic Diseases, Tohoku University Graduate School of Medicine, 2-1 Seiryo-machi, Aoba-ku, Sendai, Miyagi 980-8575, Japan, [3]Division of Stem Cell Regulation Research, Osaka University Graduate School of Medicine, Suita, Osaka 565-0871, Japan and [4]Genome Science Division, Research Center for Advanced Science and Technology, The University of Tokyo, Tokyo 153-8904, Japan

Received January 28, 2006; Revised and Accepted March 24, 2006

**Wolfram syndrome, an autosomal recessive disorder associated with diabetes mellitus and optic atrophy, is caused by mutations in the *WFS1* gene encoding an endoplasmic reticulum (ER) membrane protein. Herein, we report that pancreatic islets of *wfs1*-deficient mice exhibit increases in phosphorylation of RNA-dependent protein kinase-like ER kinase, chaperone gene expressions and active XBP1 protein levels, indicating an enhanced ER stress response. We established *wfs1*-deficient MIN6 clonal β-cells by crossing *wfs1*-deficient mice with mice expressing simian virus 40 large T antigen in β-cells. These cells show essentially the same alterations in ER stress responses as *wfs1*-deficient islets, which were reversed by re-expression of WFS1 protein or overexpression of GRP78, a master regulator of the ER stress response. In contrast, these changes are not observed in heart, skeletal muscle or brown adipose tissues with WFS1-deficiency. The increased ER stress response was accompanied by reduced BrdU incorporation and increased caspase-3 cleavage, indicating impaired cell cycle progression and accelerated apoptotic processes in the mutant islets. These changes are associated with increased expression of the cell cycle regulator $p21^{CIP1}$ in *wfs1*-deficient islets and clonal β-cells. Treatment of islets with thapsigargin, an ER stress inducer, caused upregulation of $p21^{CIP1}$. In addition, forced expression of $p21^{CIP1}$ resulted in reduced MIN6 β-cell numbers, suggesting the ER stress-induced increase in $p21^{CIP1}$ expression to be involved in β-cell loss in the mutant islets. These data indicate that WFS1-deficiency activates the ER stress response specifically in β-cells, causing β-cell loss through impaired cell cycle progression and increased apoptosis.**

## INTRODUCTION

Type 2 diabetes is caused by complex interactions between insulin resistance in peripheral tissues and impaired insulin secretion from pancreatic β-cells. There is a general consensus that the latter results from both impaired β-cell function and decreased β-cell mass (1–3). Adult β-cell mass is maintained by a balance between generation and death of β-cells. In patients with type 2 diabetes, new islet formation and β-cell replication are reportedly normal, and an increased rate of apoptosis has been suggested to underlie the loss of β-cell mass (4).

Recent studies using novel mutant mice have led to new insights into endoplasmic reticulum (ER) stress and maintenance

*To whom correspondence should be addressed. Tel: +81 227177611; Fax: +81 227177612; Email: hisamitsu-ishihara@mail.tains.tohoku.ac.jp

of β-cell mass (5,6). The ER stress response, also known as the unfolded protein response (UPR), involves translational attenuation, transcriptional induction of chaperones and folding enzymes, as well as degradation of misfolded proteins, a process called ER-associated degradation (ERAD). When ER stress is strong and cellular survival mechanisms fail to correct the protein-folding defects, an ER stress-mediated apoptotic process is initiated (5–7). Mice with a homozygous null mutation of RNA-dependent protein kinase-like ER kinase (PERK) lose their ability to phosphorylate eukaryotic initiation factor 2α (eIF2α) and fail to attenuate translation in response to ER stress. These mice develop diabetes owing to reduced β-cell mass (8). Importantly, mutations of the *EIF2AK3* gene encoding PERK in humans have been recognized as causing Wolcott-Rallison syndrome with diabetes mellitus in early infancy (9). A mouse model in which a Ser51Ala mutation of eIF2α prevents the protein from being phosphorylated by PERK and other eIF2α kinases, also displays a β-cell defect and impaired gluconeogenesis leading to lethal hypoglycemia (10). Mice with a deletion mutation of $P58^{IPK}$, a cytosolic chaperone, were recently reported to exhibit β-cell failure and diabetes (11). These examples suggest that β-cells, producing large quantities of insulin and thus a greater load on the ER, are especially sensitive to ER stress.

Wolfram syndrome is a rare autosomal recessive disorder characterized by juvenile-onset diabetes mellitus, optic atrophy, diabetes insipidus and sensorineural deafness (12). This syndrome is caused by mutations in the *WFS1* gene (13,14), which encodes an ER resident membrane protein (15). Post-mortem studies of the pancreas from subjects with Wolfram syndrome have shown β-cell loss (16). We recently established a line of mutant mice with a disrupted *wfs1* gene and found that these mice also exhibited impaired glucose homeostasis accompanied by a progressive reduction of β-cell mass (17). Thus, the *wfs1*-deficient mouse is a model for studying mechanisms of β-cell loss during the development of diabetes in Wolfram syndrome. We and others have also shown expression of WFS1 protein to be up-regulated by ER stress-inducing agents (18–20). A recent study employing IRE1α knockout and PERK knockout cells suggested that WFS1 is a component of the IRE1 and PERK signaling pathways (20). In addition, *wfs1*-deficient islets have been shown to exhibit increased DNA fragmentation in response to ER stress inducers (17), suggesting β-cell loss in Wolfram syndrome to be attributable to an inability to handle ER stress. A very recent study of islets conditionally lacking the *wfs1* gene in β-cells, demonstrated an increased GRP78 mRNA to GLUT2 mRNA ratio. This observation was interpreted as evidence of an enhanced ER stress response, on the assumption that GLUT2 mRNA levels represented the β-cell number in islets (21).

To further investigate the mechanisms underlying β-cell loss in Wolfram syndrome, we conducted a systematic study of the UPR in *wfs1*-deficient islets as well as other tissues. We also created β-cell lines with WFS1-deficiency and studied UPR. We found all three UPR subpathways to be activated in *wfs1*-deficient islets and β-cell lines. Furthermore, we demonstrated increased cleavage of caspase-3, a hallmark of apoptosis, and impaired proliferation associated with enhanced expression of the cell cycle regulator $p21^{CIP1}$.

## RESULTS

### UPR activation in *wfs1*-deficient islets

A systematic study of the UPR was conducted using islets isolated from 6-week-old male *wfs1*-deficient mice with the C57Bl/6 background. At 6 weeks of age, the β-cell mass of these mice begins to decrease (17). Accumulation of unfolded proteins in the ER is well known to induce dissociation of GRP78 from PERK, resulting in oligomerization and subsequent auto-phosphorylation of PERK. Activated PERK then phosphorylates eIF2α and suppresses general protein translation to reduce the ER load (5–7). In freshly isolated *wfs1*-deficient islets, PERK phosphorylation was increased (Fig. 1A). In addition, eIF2α phosphorylation was slightly but significantly enhanced with no alteration in total eIF2α levels in mutant islets (Fig. 1A). Thus, the ratio of phosphorylated eIF2α over total eIF2α levels analyzed by densitometry was increased by 27 ± 7% ($n = 4$ experiments, $P < 0.05$). These data indicate that one of three subpathways of the UPR arising from PERK phosphorylation is initiated in response to WFS1-deficiency in islets.

ER stress is also sensed by other ER resident proteins, IRE1 and ATF6, in addition to PERK (5–7). Activation of ATF6 via GRP78 dissociation and subsequent cleavage is known to induce the expressions of various chaperone genes, constituting another subpathway of the UPR (5–7). In *wfs1*-deficient islets, GRP94 mRNA levels were increased and those of GRP78 and $P58^{IPK}$ also tended to rise (Fig. 1B). Correspondingly, although the differences failed to reach statistical significance, levels of these chaperone proteins tended to be increased (Fig. 1C), suggesting that the ATF6 subpathway of the UPR is activated in response to WFS1-deficiency.

As shown in Figure 1D, a shorter form of XBP1 mRNA was increased. This form is produced by 26-nucleotide splicing from primary XBP1 mRNA by the ribonuclease activity of IRE1, increasing active XBP1 protein levels in mutant islets (Fig. 1E). HRD1, a ubiquitin ligase involved in ERAD, is one of the XBP1 target genes (22). In *wfs1*-deficient islets, levels of HRD1 protein were markedly increased (Fig. 1E). In addition, mRNA levels of ER-associated degradation-enhancing α-mannosidase-like protein (EDEM) (23), another target of XBP1, were significantly increased in mutant islets [100 ± 5 arbitrary units (wild-type) versus 136 ± 18 (mutant), $n = 6$, $P < 0.05$]. These data indicate that the IRE1-initiated subpathway of the UPR is also activated in *wfs1*-deficient islets.

### Establishment of MIN6 β-cell lines deficient in WFS1

To examine the influence of WFS1-deficiency specifically in a homogenous β-cell population, β-cell lines were established by crossing $wfs1^{+/-}$ and $wfs1^{-/-}$ mice (17) with IT6 mice expressing simian virus 40 (SV40) large T antigen under the insulin promoter (24) and were designated MIN6wfs1$^{+/-}$ and MIN6wfs1$^{-/-}$, respectively (see Materials and Methods). IT6 mice were previously reported to develop insulinoma, from which the MIN6 cell line (24), one of the most highly differentiated β-cell lines, was generated. We established two cell lines each for the $wfs1^{+/-}$ and $wfs1^{-/-}$ genotypes. As shown in Figure 2A, the two cell lines with the $wfs1^{-/-}$ genotype (MIN6wfs1$^{-/-}$ − 1 and 2) show similar UPR

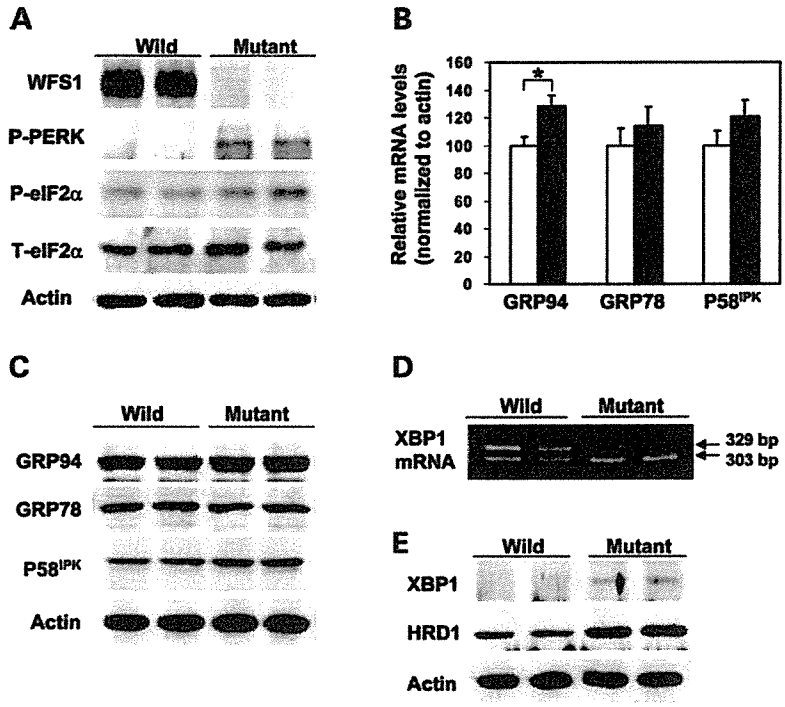


**Figure 1.** Activation of three subpathways of the UPR in *wfs1*-deficient islets. (**A**) Activation of the PERK/eIF2α pathway. Islets isolated from wild-type and *wfs1*-deficient mice were subjected to SDS–PAGE and probed with the indicated antibodies: P-PERK, phosphorylated-PERK; P-eIF2α, phosphorylated-eIF2α; T-eIF2α, total eIF2α. (**B**) Real-time RT–PCR analysis of GRP94, GRP78 and $P58^{IPK}$ gene expressions in wild-type (open columns) and *wfs1*-deficient (closed columns) mice. Relative mRNA levels were obtained after normalization to actin mRNA. $^{*}P < 0.05$, $n = 6$. (**C**) Expressions of chaperone proteins in *wfs1*-deficient islets. Lysates of isolated islets were probed with the indicated antibodies. (**D**) Increased XBP1 mRNA splicing in *wfs1*-deficient islets. Amplification of XBP1 mRNA from islet total RNA with specific primers yields spliced (303 bp) and non-spliced (329 bp) XBP1 transcripts. (**E**) Activation of the IRE1/XBP1 pathway. Lysates of isolated islets were probed with the indicated antibodies. Western blot data shown are representative of at least three experiments with different sets of samples.

characteristics. Similarly, characteristics of two cell lines with the *wfs1*$^{+/-}$ genotype (MIN6wfs1$^{+/-}$) were indistinguishable (data not shown). Therefore, only one line of each genotype was used for subsequent analyses. We compared MIN6wfs1$^{-/-}$ with MIN6wfs1$^{+/-}$ at the same passage numbers (passages 5–8), but not with the original MIN6 cells. This is because we were concerned that a difference in passage number between the original MIN6 and MIN6wfs1$^{-/-}$ cells, irrespective of WFS1-deficiency, might affect the protein expression profile, rendering the former an inappropriate control for the latter. After completion of a series of experiments, MIN6wfs1$^{+/-}$ cells reached passages 15–20, the same passage of original MIN6 cells we have. The function and survival of MIN6wfs1$^{+/-}$ cells are similar to those of wild-type MIN6 cells at similar passage numbers (data not shown).

### Effects of WFS1-deficiency on UPR in β-cell lines

As shown in Figure 2A, altered expressions of UPR-related proteins observed in *wfs1*-deficient islets were reproduced in MIN6wfs1$^{-/-}$ cells; PERK phosphorylation, as well as expressions of active XBP1 and HRD1, were increased in *wfs1*-deficient MIN6 cells. ATF4 levels were also shown to be increased in these cells. Furthermore, although GRP78 and GRP94 protein levels were similar (Fig. 2B, upper panel), the activity of the GRP78 promoter containing three ER stress response elements was greater in MIN6wfs1$^{-/-}$ cells than in MIN6wfs1$^{+/-}$ cells (Fig. 2B), strongly suggesting activation of the ATF6 subpathway of the UPR in MIN6wfs1$^{-/-}$ cells. To confirm that alterations in UPR-related proteins are due to WFS1-deficiency, wild-type human WFS1 protein was expressed in MIN6wfs1$^{-/-}$ cells. We took advantage of the tetracycline-inducible expression system. MIN6wfs1$^{-/-}$ cells were infected with the Tet-repressor expressing virus (AdCAG-TR) together with a recombinant adenovirus bearing wild-type human WFS1 cDNA under the CMV promoter containing the Tet-operator (AdCTO-WFS1). The cells were then treated with doxycycline (2 μg/ml). As shown in Figure 2C, when WFS1 expression was restored to levels comparable to those of the original MIN6 cells, the increase in PERK phosphorylation was prevented. In addition, overexpression of GRP78, a master regulator of the ER stress response, also resulted in normalization of PERK phosphorylation levels (Fig. 2D), clearly indicating the observed alteration in UPR-related proteins to be due to exacerbation of ER stress caused by WFS1-deficiency.

### No UPR induction in heart, skeletal muscle or brown adipose tissues from *wfs1*-deficient mice

WFS1 protein is expressed in a variety of non-pancreatic tissues, though less abundantly than in islets (Fig. 3A).

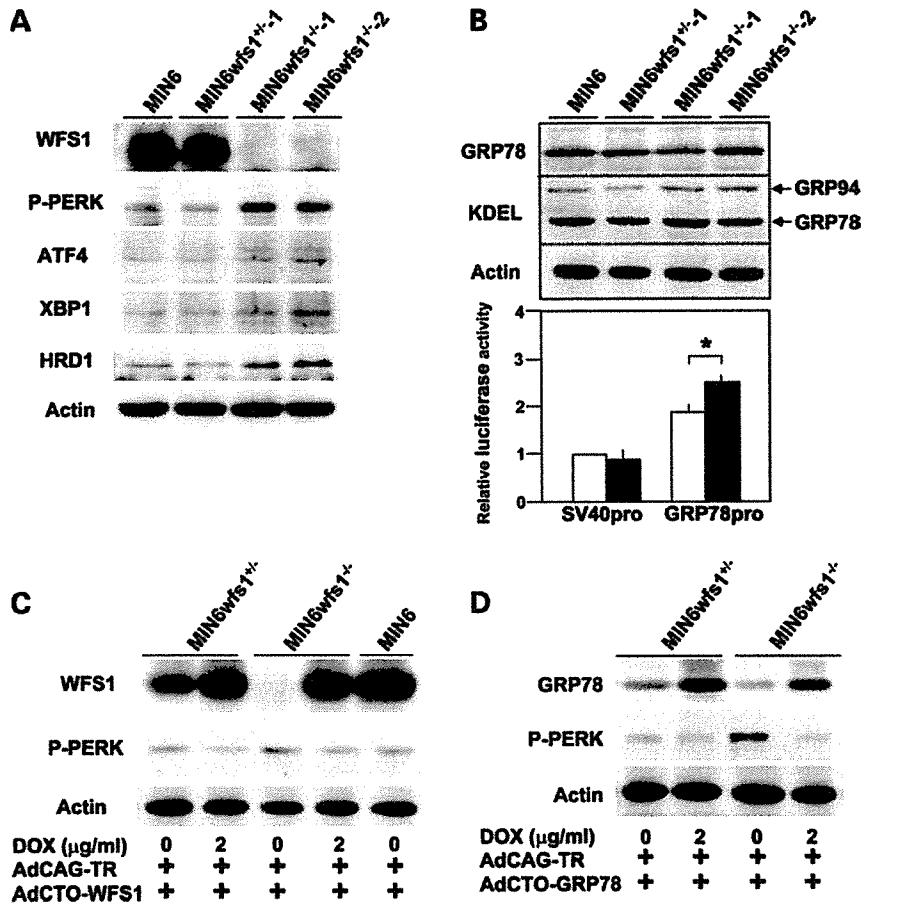


**Figure 2.** Increased UPR and its reversal by expression of WFS1 or GRP78 in an SV40 transformed *wfs1*-deficient β-cell line (MIN6wfs1$^{-/-}$). (**A**) Expression of UPR-related proteins in various MIN6 cell lines. MIN6, MIN6wfs1$^{+/-}$ – 1, MIN6wfs1$^{-/-}$ – 1 and MIN6wfs1$^{-/-}$ – 2 cells were lysed and probed with the indicated antibodies. Data shown are representative of at least three experiments with different sets of samples. (**B**) Expressions of chaperone proteins in MIN6wfs1$^{-/-}$ cells. (Upper panel) Cellular lysates were probed with anti-GRP78, anti-KDEL and anti-actin (loading control) antibodies. (Lower panel) MIN6wfs1$^{+/-}$ (open columns) and MIN6wfs1$^{-/-}$ (closed columns) cells were transiently transfected with the pGL3-promoter plasmid containing the SV40 promoter-luciferase (SV40pro: 0.5 μg) or pGRP78pro(−172)-Luc (GRP78pro: 0.5 μg) together with the reference plasmid pTK-RL (0.05 μg) encoding *Renilla* luciferase. Twenty-four hours after transfection, cellular lysates were subjected to luciferase assay. The luciferase activity of the pGL3-promoter in MIN6wfs1$^{+/-}$ was defined as 1. The averages of three independent experiments, each performed in duplicate, are presented. *$P < 0.05$, $n = 3$. (**C**) Suppression of PERK phosphorylation by WFS1 re-expression in MIN6wfs1$^{-/-}$ cells. Cells were infected with AdCAG-TR expressing Tet-repressor and AdCTO-WFS1 harboring *WFS1* cDNA. WFS1 expression was induced by 48 h doxycycline (DOX, 2 μg/ml) treatment. The experiment was repeated three times and similar results were obtained. (**D**) Suppression of PERK phosphorylation by GRP78 overexpression in MIN6wfs1$^{-/-}$ cells. Human GRP78 expression was induced by 48 h DOX treatment. The experiment was repeated four times and similar results were obtained.

Therefore, we also examined expressions of UPR genes in tissues other than pancreatic islets. Cardiac function is reportedly not impaired in subjects with Wolfram syndrome (12) or in *wfs1*-deficient mice (17). Skeletal muscle and brown adipose tissue also appear essentially normal in mutant mice (data not shown). In contrast to islets, no UPR alterations were observed in these tissues from *wfs1*-deficient mice (Fig. 3B–D). Thus, UPR activation is tissue-specific in WFS1-deficiency.

### Increased β-cell apoptotic response in *wfs1*-deficient islets

ER stress induces apoptosis through activation of various signaling molecules including JNK and pro-apoptotic proteins, such as CHOP (5–7). CHOP expression was increased at both the mRNA (Fig. 4A) and the protein level (Fig. 4B), in mutant when compared with wild-type islets. In contrast, JNK expression levels and phosphorylation states were not altered in *wfs1*-deficient islets (Fig. 4B). We also found increased levels of cleaved caspase-3, a hallmark of apoptosis, in mutant islets (Fig. 4B). CHOP expression and cleaved caspase-3 levels were also increased in *wfs1*-deficient MIN6 cells (Fig. 4C), whereas no such changes were observed in heart, skeletal muscle or adipose tissue (data not shown).

We also measured apoptosis in MIN6wfs1$^{-/-}$ and MIN6wfs1$^{+/-}$ cells by counting adherent cells positive for annexin V staining under fluorescent microscope. We found 1–2% cells to be annexin V positive for both the *wfs1*$^{-/-}$ and the *wfs1*$^{+/-}$ genotype cultured under standard conditions, i.e. no differences between MIN6wfs1$^{-/-}$ and MIN6wfs1$^{+/-}$

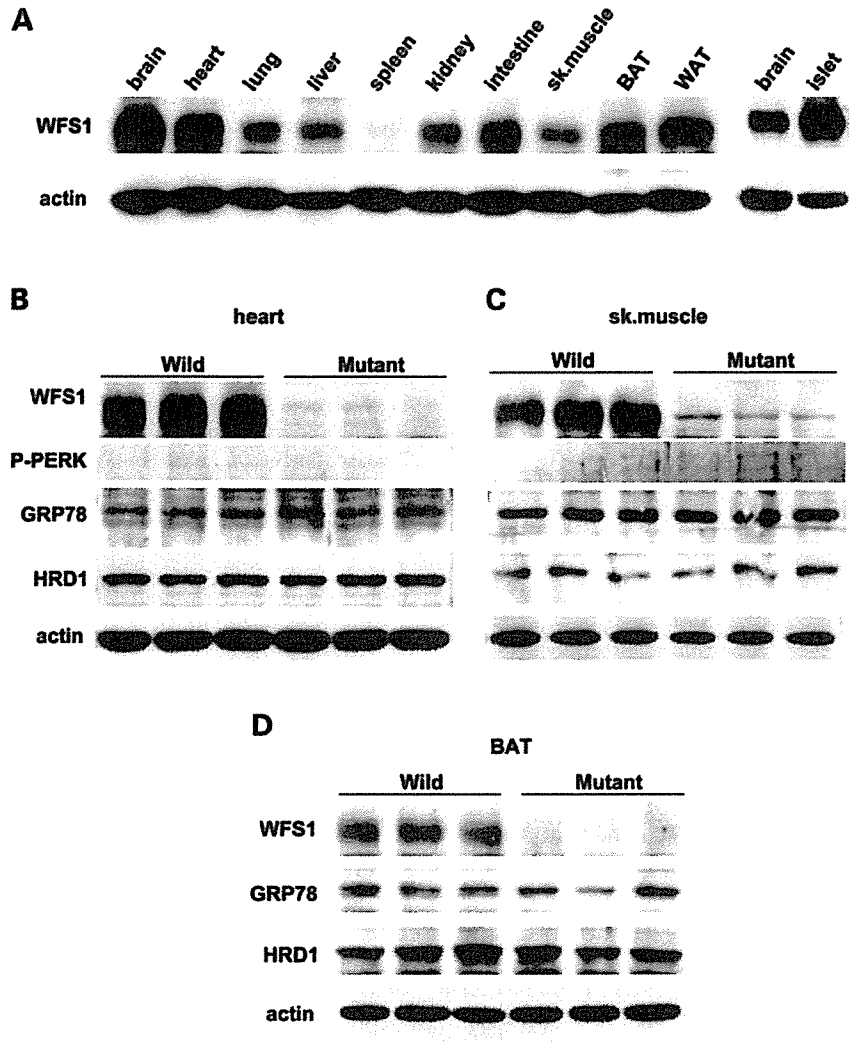


**Figure 3.** No UPR changes in heart, skeletal muscle or brown adipose tissue from *wfs1*-deficient mice. (**A**) WFS1 protein distribution in mice. Approximately, 100 μg of protein from wild-type mouse tissues were analyzed for the presence of WFS1 protein. BAT, brown adipose tissue; WAT, white adipose tissue. (**B–D**) UPR activation was not observed in heart (B), skeletal muscle (C) or BAT (D) from *wfs1*-deficient mice. The western blot data shown are representative of two experiments, each performed using three mice of each genotype.

cells. An increase in the number of apoptotic cells was observed when MIN6wfs1$^{-/-}$ cells were challenged with 0.5 μM thapsigargin (TG) for 24 h, as compared with MIN6wfs1$^{+/-}$ cells under the same conditions [2.7 ± 1.0% (MIN6wfs1$^{+/-}$) versus 6.2 ± 1.1% (MIN6wfs1$^{-/-}$) $n = 3$, $P < 0.05$]. Therefore, MIN6wfs1$^{-/-}$ cells exhibited increased apoptosis susceptibility. These data, together, indicate that an ER stress mediated-apoptotic process is activated in *wfs1*-deficient β-cells.

### Impaired β-cell proliferation in *wfs1*-deficient islets

In addition to increased apoptosis, decreased proliferation may contribute to loss of β-cell mass in *wfs1*-deficient mice. When β-cell proliferation activity was assayed by 5-bromodeoxyuridine (BrdU) incorporation in pancreases from wild-type and mutant mice, BrdU incorporation was found to be significantly reduced in *wfs1*-deficient β-cells (Fig. 5A and B). This observation suggested impaired proliferation, along with increased apoptosis, to contribute to β-cell loss in *wfs1*-deficient islets.

We next explored possible causes of the decreased β-cell proliferation in *wfs1*-deficient islets. The link between the UPR and cell cycle arrest was previously reported to be mediated by down-regulation of cyclin D1 because of general translational suppression via eIF2α phosphorylation (25). However, neither expression of cyclin D1 nor that of cyclin D2, major isoforms of the D type cyclins in β-cells (26,27), was changed in mutant islets (data not shown). CHOP has also been recognized as causing cell cycle arrest and apoptosis (28,29). As GADD34 is reportedly a target of CHOP (30) and is involved in cell growth and survival (31),

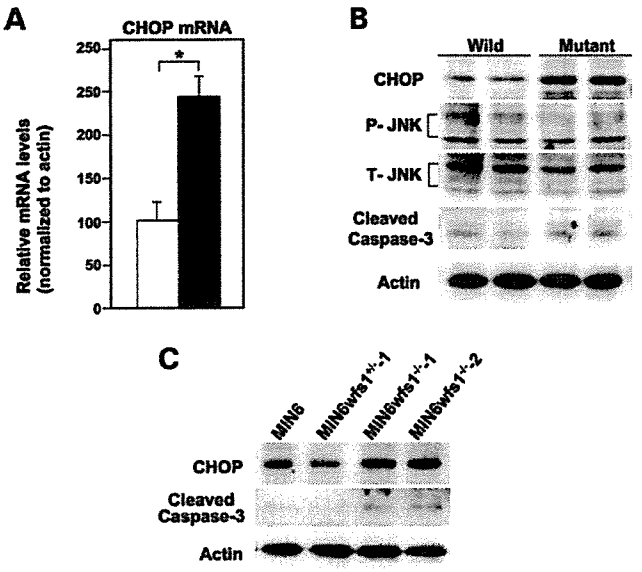


**Figure 4.** Activation of apoptosis signaling in *wfs1*-deficient islets and MIN6 cells. (**A**) Real-time RT–PCR analysis of CHOP mRNA in wild-type (open column) and *wfs1*-deficient (closed column) islets. Relative mRNA levels were obtained after normalization to actin mRNA. $^{*}P < 0.05$, $n = 6$. (**B**) Western blot analysis of apoptosis signaling proteins in *wfs1*-deficient islets. Lysates of islets were probed with the indicated antibodies: P-JNK, phospho-JNK; T-JNK, total-JNK. Data shown are representative of three experiments with different sets of samples. (**C**) Increased expression of CHOP and cleaved caspase-3 in *wfs1*-deficient MIN6 cells. Lysates of MIN6 cell derivatives were probed with the indicated antibodies. Data shown are representative of three experiments.

GADD34 expression was examined. GADD34 transcript levels were found to be increased in *wfs1*-deficient islets ($100 \pm 11$ versus $151 \pm 14$, $P < 0.05$). Recent studies have demonstrated that cell cycle regulation is critical for maintenance of β-cell mass (25,26). As GADD34 reportedly induces p53 phosphorylation and enhances expression of the cell cycle inhibitor $p21^{CIP1}$ (32), p53 and $p21^{CIP1}$ expressions were assessed. We found phosphorylation of p53 to be increased, though total p53 was not elevated (Fig. 5C). In addition, increased expressions of $p21^{CIP1}$ mRNA ($100 \pm 11$ versus $413 \pm 32$, $P < 0.01$) and $p21^{CIP1}$ protein (Fig. 5C) were observed in *wfs1*-deficient islets. We also examined the expression of another cell cycle inhibitor, $p27^{KIP1}$, and found no difference between wild-type and mutant islets (Fig. 5C). Increased expression of $p21^{CIP1}$ protein was also observed in *wfs1*-deficient MIN6 cells, SV40 large T antigen-transformed cells in which p53 activity was considered to be suppressed (Fig. 5D). Expression of $p21^{CIP1}$ protein was not increased in heart, skeletal muscle or brown adipose tissues from *wfs1*-deficient mice (data not shown).

In order to determine whether increased expression of $p21^{CIP1}$ is attributable to ER stress, wild-type islets were treated with TG (0.5 μM) for 12 h. As shown in Figure 5E, expression of $p21^{CIP1}$ was significantly increased. In addition, expression of $p21^{CIP1}$ was markedly increased in MIN6 cells treated with TG (Fig. 5F) or tunicamycin (data not shown). These data suggest $21^{CIP1}$ expression to be induced by ER stress in β-cells.

Finally to assess the effects of $p21^{CIP1}$ expression on β-cell proliferation, $p21^{CIP1}$ was expressed in wild-type MIN6 cells in a tetracycline-inducible manner (Fig. 6A). Overexpression of $p21^{CIP1}$ suppressed a MIN6 cell number increase (Fig. 6B), suggesting that increased $p21^{CIP1}$ expression contributes to the reduced β-cell mass in *wfs1*-deficient islets.

## DISCUSSION

We systematically investigated UPR in *wfs1*-deficient islets and MIN6 β-cells as well as heart, skeletal muscle and brown adipose tissues from the mutant mice in this study. Enhanced UPR was specifically observed in β-cells but not in other tissues examined. These findings indicate that diabetes in Wolfram syndrome is caused by increased ER stress in β-cells and establish Wolfram syndrome as an ER stress-based disease, as is the case in Wolcott-Rallison syndrome with PERK-deficiency (9). Furthermore, we found enhanced UPR to be associated with not only activation of the apoptotic pathway but also impaired cell cycle progression in β-cells. These observations provide evidence of novel mechanisms underlying ER stress-mediated β-cell loss.

We demonstrated activation of the PERK and IRE1 subpathways of the UPR. Increased activation of the GRP78 promoter indicates the ATF6 subpathway to be induced as well. GRP78 expression was also reportedly increased by knockdown of WFS1 expression in INS1 insulinoma β-cells (20). Collectively, these data indicate that all three UPR subpathways are activated by WFS1-deficiency in β-cells. The UPR is activated when ER homeostasis is perturbed by defective ER calcium homeostasis, mutations in ER resident proteins and/or abnormalities of the ERAD system. Disturbed ER homeostasis is also induced by defect(s) in components of the UPR system, as is the case in Wolcott-Rallison syndrome with PERK-deficiency. The present data suggest that impaired ER homeostasis does not result from defect(s) in a specific pathway(s) of the UPR. Our previous study demonstrated an abnormal cytosolic $Ca^{2+}$ response in *wfs1*-deficient β-cells (17), suggesting that impaired ER $Ca^{2+}$ homeostasis is a possible cause of ER stress associated with WFS1-deficiency.

We found that WFS1 protein is highly expressed in heart, skeletal muscle and brown adipose tissues. However, there is no UPR activation in these tissues from mutant mice. Thus, the UPR is tissue-specific in *wfs1*-deficient mice. One possible explanation of this tissue specificity is that a protein(s), compensating for loss of WFS1 protein function is present in these tissues but not in β-cells. This interesting possibility merits further investigation and elucidation of WFS1 function is necessary to resolve the tissue-specific effects of WFS1-deficiency.

Our results demonstrate, in addition to the augmented apoptotic process evidenced by increased caspase-3 cleavage, that β-cell proliferation is decreased in *wfs1*-deficient mice. Impaired proliferation was also reported in BRIN-BD11 cells expressing the human WFS1 antisense transcript (33). Our observation is in contrast to that by Riggs *et al.* (21) who detected no changes in the numbers of BrdU-positive cells in islets from β-cell specific *wfs1* knockout mice. The reason for this discrepancy is currently unclear, but may

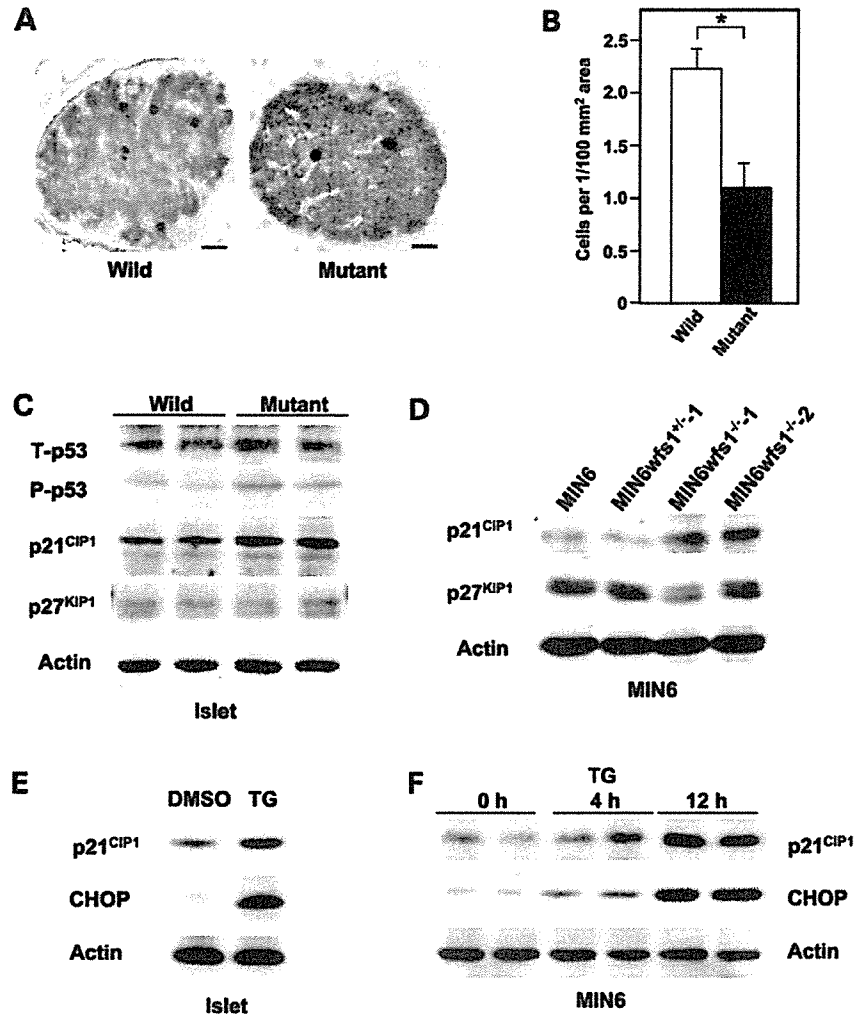


**Figure 5.** Impaired cell cycle progression and increased $p21^{CIP1}$ expression in *wfs1*-deficient islets. (**A** and **B**) Impaired cell cycle progression in *wfs1*-deficient β-cells. Incorporated BrdU and insulin were probed with specific antibodies (A) and BrdU positive β-cells were counted (B). Bars, 10 μM. $^*P < 0.05$, $n = 4$ mice per group. (**C** and **D**) Increased $p21^{CIP1}$ expression in *wfs1*-deficient islets and MIN6 cells. Lysates of wild-type and *wfs1*-deficient islets (C) or MIN6 cells (D) were probed with the indicated antibodies: T-p53, total-p53; P-p53, phospho-p53. Data shown are representative of three experiments with different sets of samples. (**E** and **F**) Induction of $p21^{CIP1}$ expression by TG in islets (E) and MIN6 cells (F). Wild-type islets were challenged with 0.5 μM TG for 12 h. MIN6 cells were also treated with 0.5 μM TG for the indicated durations. Lysates of islets or MIN6 cells were probed with the indicated antibodies. The experiment was repeated three times and similar results were obtained.

reflect differences in the ages of the mice studied: 6-week-old mice were used in the present versus 12- or 24-week-old animals in their study (21). Cell cycle dysregulation in *wfs1*-deficient islets was associated with increased expression of $p21^{CIP1}$, a cell cycle regulator. $p21^{CIP1}$ can serve, depending on which tissues or cells it is activated in, as both an inhibitor and an agonist of cell cycle progression (34). Our observation that forced expression of $p21^{CIP1}$ suppressed MIN6 β-cell proliferation suggests that $p21^{CIP1}$ operates as a cell cycle inhibitor in β-cells, although our results must be interpreted cautiously, as forced overexpression of $p21^{CIP1}$ may produce effects different from those occurring in mutant β-cells with increased $p21^{CIP1}$ levels. A very recent study, demonstrating that $p21^{CIP1}$ acts as a molecular brake on mitogenic stimuli in β-cells (35), supports the notion of $p21^{CIP1}$ functioning as a cell cycle inhibitor in β-cells. ER stress inducers were recently reported to cause $p21^{CIP1}$ expression and cell cycle arrest in chondrocytes (36) and prostatic cancer cells (37), suggesting that cell cycle arrest associated with increased $p21^{CIP1}$ expression is a common feature in cells under ER stress. Furthermore, reduced proliferation associated with increased expression of $p21^{CIP1}$, in *wfs1*-deficient β-cells (the present study) and β-cells transgenic for hepatocyte growth factor and/or placental lactogen (35), highlights an important role for $p21^{CIP1}$ in regulation of β-cell mass in addition to the roles of $p27^{KIP1}$ recently reported (38).

CHOP induces GADD34 expression (30), which then activates p53 phosphorylation and $p21^{CIP1}$ transcription (32). Therefore, the CHOP → GADD34 → p53 pathway is a candidate for ER stress-mediated $p21^{CIP1}$ expression. Indeed,

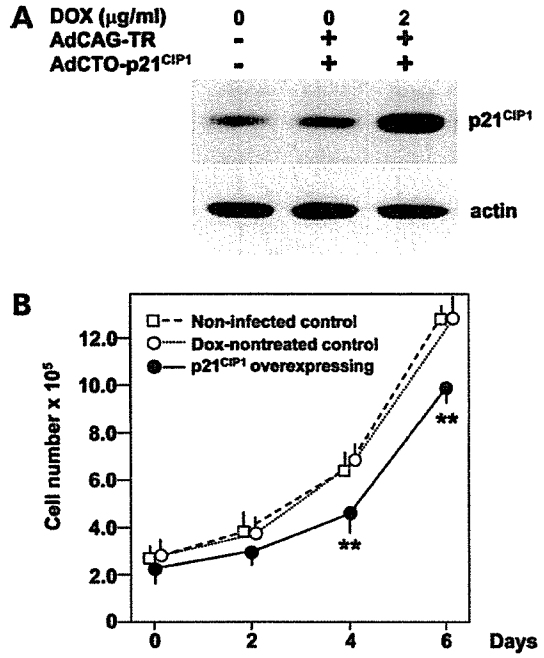


**Figure 6.** Decrease in MIN6 cell numbers in response to forced $p21^{CIP1}$ expression. (**A**) Forced expression of $p21^{CIP1}$ in MIN6 cells. Cells were either uninfected or infected with AdCAG-TR (m.o.i. of 30) and AdCTO-$p21^{CIP1}$ (m.o.i. of 100) harboring $p21^{CIP1}$ cDNA. Expression of $p21^{CIP1}$ was induced by 48 h DOX (2 μg/ml) treatment. MIN6 cell lysates were subjected to immunoblot analysis using anti-$p21^{CIP1}$ and actin antibodies. (**B**) Numbers of MIN6 cells overexpressing $p21^{CIP1}$. One day after adenovirus transduction, cells were reseeded ($2 \times 10^5$ per well) and divided into two groups, and, after two more days, treatment with (closed circles) or without (open circles) DOX (2 μg/ml) was commenced (day 0). Uninfected MIN6 cells (open squares) were also seeded 2 days before. Cells were then harvested on days 0, 2, 4 and 6, stained with trypan blue and counted. Data are means ± S.E. for triplicate wells. $^{**}P < 0.01$ against both controls. The experiment was repeated three times and similar results were obtained.

an increase in $p21^{CIP1}$ expression was associated with increased GADD34 expression and p53 phosphorylation in *wfs1*-deficient β-cells. However, induction of $p21^{CIP1}$ expression by TG was observed in MIN6 cells transformed with SV40 large T antigen, a well-known suppressor of p53. In addition, an ER stress-induced increase in $p21^{CIP1}$ expression was observed in p53-deficient prostatic cancer cells (37). Thus, ER stress appears to induce $p21^{CIP1}$ expression through both p53-dependent and -independent mechanisms.

As β-cells are apparently much more sensitive to ER stress than other types of cells and tissues (39), ER stress might be a more common cause of β-cell failure than previously thought, especially in terms of the increased insulin demands of modern lifestyles. Our data indicate that both increased apoptosis and impaired proliferation, in β-cells, are mechanisms leading to β-cell loss in *wfs1*-deficient islets, a model of ER-stress mediated β-cell failure. Further studies designed to elucidate the molecular mechanisms of β-cell loss under chronic ER stress are anticipated to contribute to future treatments for type 2 diabetes.

## MATERIALS AND METHODS

### Antibodies

The monoclonal antibody against $P58^{IPK}$ was a generous gift from Prof. M.G. Katze (University of Washington). Other antibodies were purchased from the indicated sources: anti-GRP94, anti-KDEL (Stressgen Biotechnologies), anti-GRP78, anti-XBP1, anti-$p21^{CIP1}$, anti-CHOP, anti-p53, anti-phosphorylated p53 and anti-ATF4 (Santa Cruz Biotechnology), anti-HRD1 (Abgent), anti-phosphorylated PERK, anti-JNK, anti-phosphorylated JNK, anti-eIF2α, anti-phosphorylated eIF2α, and anti-cleaved caspase-3 (Cell Signaling), and anti-$p27^{KIP1}$ (BD Transduction Laboratories).

### Mouse islet isolation, real-time RT–PCR and western blot

The *wfs1*-deficient mice used had a C57Bl/6 background and were described previously (17). All animal experiments were approved by the Tohoku University Institutional Animal Care and Use Committee (#15–45). Islets were isolated by collagenase infusion through the common bile duct and harvested by hand. Total RNA was prepared immediately after islet isolation using an RNAeasy kit (Qiagen). For real-time RT–PCR analysis, cDNA was synthesized by reverse transcription using the oligo $d(T)_{16}$ primer and subjected to PCR amplification with gene-specific primers (Table 1) using a SYBR Green 1 kit (Roche). Data are presented as relative values to actin mRNA. For detection of the spliced form of XBP1 mRNA, the primers were: 5′-TGAGAACCAGGA GTTAAGAAACGC-3′ and 5′-TTCTGGGTAGACCTCTGG GAGTTCC-3′. For immunoblotting, islets from three to four mice were pooled, dissolved immediately after isolation in a lysis buffer (~100 islets/15 μl) and subjected to SDS–polyacrylamide gel electrophoresis. In several experiments, isolated islets were cultured overnight and treated with 0.5 μM TG for 12 h. All western blot experiments were repeated at least three times, with different sets of samples, throughout this study. Immunoblot band intensities were analyzed using Scion image software (Scion Corporation) and normalized with those of actin.

### Establishment of MIN6wfs1$^{-/-}$ and MIN6wfs1$^{+/-}$ cell lines

The *wfs1*$^{-/-}$ mice (17) were bred with IT6 mice expressing SV40 large T antigen under the human insulin promoter (24) and the resulting *wfs1*$^{+/-}$:SV40Tag/+ mice were further bred with *wfs1*$^{-/-}$ mice. Tumors from pancreases of 10- to 12-week-old *wfs1*$^{+/-}$:SV40Tag/+ and *wfs1*$^{-/-}$: SV40Tag/+ mice were carefully excised and placed in Dulbecco's Modified Eagle's Medium containing penicillin and streptomycin. Cells were expanded and frozen at passages 3 and 4. We used these cells at 5–8 passages in this study. For study of apoptosis, MIN6 cells were infected with AdRI-PeGFP expressing enhanced green fluorescent protein under the insulin promoter to facilitate detection of cells under fluorescent microscope. Apoptosis was examined by staining with annexin V using the Annexin V-Cy3 apoptosis detection kit

**Table 1.** Primers used for quantitative real-time RT–PCR

| Genes | Forward | Reverse |
|---|---|---|
| *ATF4* | 5′-TCCTGAACAGCGAAGTGTTG-3′ | 5′-ACCCATGAGGTTTCAAGTGC-3′ |
| *GRP94* | 5′-TGATGAAGTCGACGTGGATG-3′ | 5′-TCCTGTTCACTTCAGCTTGG-3′ |
| *GRP78* | 5′-GACATTTGCCCAGAAGAAA-3′ | 5′-CTCATGACATTCAGTCCAGCA-3′ |
| *P58$^{IPK}$* | 5′-CCTTATCGGACAGTCCTTCG-3′ | 5′-TCAGAGTCCTGATTTCATCTTCA-3′ |
| *EDEM* | 5′-GGAAATTCATCCGAGTTCCA-3′ | 5′-GGGCCATGTACAACAATTCA-3′ |
| *CHOP* | 5′-CCTAGCTTGGCTGACAGAGG-3′ | 5′-CTGCTCCTTCTCCTTCATGC-3′ |
| *GADD34* | 5′-CGGAGAGAAGCCAGAATCAC-3′ | 5′-CAGCAAGGAAATGGACTGTG-3′ |
| *P21$^{CIP1}$* | 5′-ACATCTCAGGGCCGAAAAC-3′ | 5′-CCTGACCCACAGCAGAAGAG-3′ |

(Medical and Biological Laboratories). At least 1000 cells per sample were counted for annexin V positive cells.

### GRP78 promoter assay

The pGL3-promoter, pTK-RLuc and pGL3-basic plasmids were purchased from Promega. The mouse GRP78 promoter fragment spanning −172 to −21 (positions relative to the transcription start site) was amplified by PCR using oligonucleotides 5′-GACTCGAGGCCGCTTCGAATCGGCAG-3′ and 5′-TCAAGCTTGGCCAGTATCGAGCGCGC-3′. This fragment contains three ER stress response elements (40) and the corresponding regions of human (40) and rat (41) *GRP78* genes were shown to respond to ATF6 activation. A GRP78 promoter-driving luciferase reporter plasmid (designated pmGRP78pro(−172)-Luc) was constructed by subcloning this fragment into the *Xho*I and *Hind*III sites of the pGL3-basic vector. MIN6wfs1$^{+/-}$ or MIN6wfs1$^{-/-}$ cells were co-transfected with pGL3-promoter or pGRP78pro(−172)-Luc together with pTK-RLuc using the LipofectAMINE reagent (Invitrogen). Luciferase activities were assayed with Dual-Luciferase reporter system (Promega) using a Lumat LB9507 luminometer (Berthold).

### BrdU incorporation assay

BrdU (100 mg/kg) was injected into the mice intraperitoneally. Six hours later, the mice were sacrificed and their pancreases were fixed with 4% paraformaldehyde. Immunohistochemical analyses were performed with a Cell Proliferation Assay kit (BD Pharmingen). Sections were also stained with anti-insulin. BrdU-positive β-cells were counted in at least 50 sections per mouse.

### Recombinant adenovirus experiments

Human *GRP78* cDNA was purchased from Open Biosystems. Human *WFS1* cDNA was a generous gift from Prof. Y. Tanizawa (Yamaguchi University). The CMV promoter containing two Tet-operator sequences (designated CTO) was excised from pcDNA5/TO (Invitrogen) and ligated to these cDNAs. The Tet-repressor cDNA was excised from pcDNA6/TR (Invitrogen) and ligated to the CAG promoter unit (42). These expression units were used to generate recombinant adenoviruses by a previously described method (43). The resulting viruses were designated AdCAG-TR for the Tet-repressor expressing virus and AdCTO-GRP78 for the GRP78 expressing virus under the CTO promoter, and so on. MIN6 and its derivative cells were infected with AdCAG-TR at a multiplicity of infection (m.o.i.) of 30 together with viruses with the CTO promoter at an m.o.i. of 100. One day after infection, cells were reseeded and divided into two groups. Two days thereafter, the cells were fed media with or without doxycycline (2 μg/ml). We have observed no adverse effects of infection of a control recombinant adenovirus expressing green fluorescence protein at an m.o.i. of less than 250 on MIN6 cell function in terms of cell proliferation and glucose-stimulated insulin secretion (data not shown). For the cell number assessment, MIN6 cells infected with AdCAG-TR and AdCTO-p21$^{CIP1}$ were seeded in six-well plates at $2 \times 10^5$ per well, cultured in media with or without doxycycline (2 μg/ml) and harvested after the indicated intervals. Cells were then stained with trypan blue and counted.

### Statistical analysis

Data are presented as means ± S.E. Differences between groups were assessed by Student's *t*-test.

## ACKNOWLEDGEMENTS

We thank Profs. M.G. Katze and Y. Tanizawa for their generous gifts of the monoclonal antibody against P58$^{IPK}$ and human WFS1 cDNA, respectively. We are also grateful to Y. Nagura and K. Tanaka for their expert assistance. This research was supported by Grants-in-Aid for Scientific Research (17590264 to H.I. and 17390258 to Y.O.) from the Ministry of Education, Science, Sports and Culture of Japan.

*Conflict of Interest statement.* None declared.

## REFERENCES

1. Donath, M.Y. and Halban, P.A. (2004) Decreased beta-cell mass in diabetes: significance, mechanisms and therapeutic implications. *Diabetologia*, **47**, 581–589.
2. Rhodes, C.J. (2005) Type 2 diabetes–a matter of beta-cell life and death? *Science*, **307**, 380–384.
3. Porter, J.R. and Barrett, T.G. (2005) Monogenic syndromes of abnormal glucose homeostasis: clinical review and relevance to the understanding of the pathology of insulin resistance and beta cell failure. *J. Med. Genet.*, **42**, 893–902.
4. Butler, A.E., Janson, J., Bonner-Weir, S., Ritzel, R., Rizza, R.A. and Butler, P.C. (2003) Beta-cell deficit and increased beta-cell apoptosis in humans with type 2 diabetes. *Diabetes*, **52**, 102–110.

5. Harding, H.P. and Ron, D. (2002) Endoplasmic reticulum stress and the development of diabetes: a review. *Diabetes*, **51** (Suppl. 3), S455–S461.
6. Wu, J. and Kaufman, R.J. (2006) From acute ER stress to physiological roles of the unfolded protein response. *Cell Death Differ.*, **13**, 374–384.
7. Schroder, M. and Kaufman, R.J. (2005) The mammalian unfolded protein response. *Annu. Rev. Biochem.*, **74**, 739–789.
8. Harding, H.P., Zhang, Y., Zeng, H., Jungries, R., Chung, P., Plesken, H., Sabatini, D.D. and Ron, D. (2001) Diabetes mellitus and exocrine pancreatic dysfunction in perk−/− mice reveals a role for translational control in secretory cell survival. *Mol. Cell*, **7**, 1153–1163.
9. Delepine, M., Nicolino, M., Barrett, T., Golamaully, M., Lathrop, G.M. and Julier, C. (2000) *EIF2AK3*, encoding translation initiation factor 2-alpha kinase 3, is mutated in patients with Wolcott-Rallison syndrome. *Nat. Genet.*, **25**, 406–409.
10. Scheuner, D., Song, B., McEwen, E., Liu, C., Laybutt, R., Gillespie, P., Saunders, T., Bonner-Weir, S. and Kaufman, R.J. (2001) Translational control is required for the unfolded protein response and *in vivo* glucose homeostasis. *Mol. Cell*, **7**, 1165–1176.
11. Ladiges, W.C., Knoblaugh, S.E., Morton, J.F., Korth, M.J., Sopher, B.L., Baskin, C.R., MacAuley, A., Goodman, A.G., LeBoeuf, R.C. and Katze, M.G. (2005) Pancreatic β-cell failure and diabetes in mice with a deletion mutation of the endoplasmic reticulum molecular chaperone gene $P58^{IPK}$. *Diabetes*, **54**, 1074–1081.
12. Wolfram, D.J. and Wagener, H.P. (1938) Diabetes mellitus and simple optic atrophy among siblings: report on four cases. *Mayo Clinic Proc.*, **13**, 715–718.
13. Inoue, H., Tanizawa, Y., Wasson, J., Behn, P., Kalidas, K., Bernal-Mizrachi, E., Mueckler, M., Marshall, H., Donis-Keller, H., Crock, P. *et al.* (1998) A gene encoding a transmembrane protein is mutated in patients with diabetes mellitus and optic atrophy (Wolfram syndrome). *Nat. Genet.*, **20**, 143–148.
14. Strom, T.M., Hortnagel, K., Hofmann, S., Gekeler, F., Scharfe, C., Rabl, W., Gerbitz, K.D. and Meitinger, T. (1998) Diabetes insipidus, diabetes mellitus, optic atrophy and deafness (DIDMOAD) caused by mutations in a novel gene (wolframin) coding for a predicted transmembrane protein. *Hum. Mol. Genet.*, **7**, 2021–2028.
15. Takeda, K., Inoue, H., Tanizawa, Y., Matsuzaki, Y., Oba, J., Watanabe, Y., Shinoda, K. and Oka, Y. (2001) *WFS1* (Wolfram syndrome 1) gene product: predominant subcellular localization to endoplasmic reticulum in cultured cells and neuronal expression in rat brain. *Hum. Mol. Genet.*, **10**, 477–484.
16. Karasik, A., O'hara, C., Srikanta, S., Swift, M., Soeldner, J.S., Kahn, C.R. and Herskowitz, R.D. (1989) Genetically programmed selective islet beta-cell loss in diabetic subjects with Wolfram's syndrome. *Diab. Care*, **12**, 135–138.
17. Ishihara, H., Takeda, S., Tamura, A., Takahashi, R., Yamaguchi, S., Takei, D., Yamada, T., Inoue, H., Soga, H., Katagiri, H. *et al.* (2004) Disruption of the *wfs1* gene in mice causes progressive beta-cell loss and impaired stimulus-secretion coupling in insulin secretion. *Hum. Mol. Genet.*, **13**, 1159–1170.
18. Yamaguchi, S., Ishihara, H., Tamura, A., Yamada, T., Takahashi, R., Takei, D., Katagiri, H. and Oka, Y. (2004) Endoplasmic reticulum stress and *N*-glycosylation modulate expression of WFS1 protein. *Biochem. Biophys. Res. Commun.*, **325**, 250–256.
19. Ueda, K., Kawano, J., Takeda, K., Yujiri, T., Tanabe, K., Anno, T., Akiyama, M., Nozaki, J., Yoshinaga, T., Koizumi, A. *et al.* (2005) Endoplasmic reticulum stress induces *Wfs1* gene expression in pancreatic β cells via transcriptional activation. *Eur. J. Endocr.*, **153**, 167–176.
20. Fonseca, S.G., Fukuma, M., Lipson, K.L., Nguyen, L.X., Allen, J.R., Oka, Y. and Urano, F. (2005) WFS1 is a novel component of the unfolded protein response and maintains homeostasis of the endoplasmic reticulum in pancreatic β-cells. *J. Biol. Chem.*, **280**, 39609–39615.
21. Riggs, A.C., Bernal-Mizrachi, E., Ohsugi, M., Wasson, J., Fatrai, S., Welling, C., Murray, J., Schmidt, R.E., Herrera, P.L. and Permutt, M.A. (2005) Mice conditionally lacking the Wolfram gene in pancreatic islet beta cells exhibit diabetes as a result of enhanced endoplasmic reticulum stress and apoptosis. *Diabetologia*, **48**, 2313–2321.
22. Kaneko, M., Ishiguro, M., Niinuma, Y., Uesugi, M. and Nomura, Y. (2002) Human HRD1 protects against ER stress-induced apoptosis through ER-associated degradation. *FEBS Lett.*, **532**, 147–152.
23. Hosokawa, N., Wada, I., Hasegawa, K., Yorihuzi, T., Tremblay, L.O., Herscovics, A. and Nagata, K. (2001) A novel ER alpha-mannosidase-like protein accelerates ER-associated degradation. *EMBO Rep.*, **2**, 415–422.
24. Miyazaki, J., Araki, K., Yamato, E., Ikegami, H., Asano, T., Shibasaki, Y., Oka, Y. and Yamamura, K. (1990) Establishment of a pancreatic β cell line that retains glucose-inducible insulin secretion: special reference to expression of glucose transporter isoforms. *Endocrinology*, **127**, 126–132.
25. Brewer, J.W. and Diehl, J.A. (2000) PERK mediates cell-cycle exit during the mammalian unfolded protein response. *Proc. Natl Acad. Sci. USA*, **97**, 12625–12630.
26. Georgia, S. and Bhushan, A. (2004) Beta cell replication is the primary mechanism for maintaining postnatal beta cell mass. *J. Clin. Invest.*, **114**, 963–968.
27. Kushner, J.A., Ciemerych, M.A., Sicinska, E., Wartschow, L.M., Teta, M., Long, S.Y., Sicinski, P. and White, M.F. (2005) Cyclins D2 and D1 are essential for postnatal pancreatic beta-cell growth. *Mol. Cell. Biol.*, **25**, 3752–3762.
28. Barone, M.V., Crozat, A., Tabaee, A., Philipson, L. and Ron, D. (1994) CHOP (GADD153) and its oncogenic variant, TLS-CHOP, have opposing effects on the induction of G1/S arrest. *Genes Dev.*, **8**, 453–464.
29. Kim, D.-G., You, K.-R., Liu, M.-J., Choi, Y.-K. and Won, Y.-S. (2002) GADD153-mediated anticancer effects of *N*-(4-hydroxyphenyl)retinamide on human hepatoma cells. *J. Biol. Chem.*, **277**, 38930–38938.
30. Marciniak, S.J., Yun, C.Y., Oyadomari, S., Novoa, I., Zhang, Y., Jungreis, R., Nagata, K., Harding, H.P. and Ron, D. (2004) CHOP induces death by promoting protein synthesis and oxidation in the stressed endoplasmic reticulum. *Genes Dev.*, **18**, 3066–3077.
31. Hollander, M.C., Poola-Kella, S. and Fornace, A.J., Jr (2003) Gadd34 functional domains involved in growth suppression and apoptosis. *Oncogene*, **22**, 3827–3832.
32. Yagi, A., Hasegawa, Y., Xiao, H., Haneda, M., Kojima, E., Nishikimi, A., Hasegawa, T., Shimokata, K. and Isobe, K. (2003) GADD34 induces p53 phosphorylation and p21/WAF1 transcription. *J. Cell. Biochem.*, **90**, 1242–1249.
33. McBain, S.C. and Morgan, N.G. (2003) Functional effects of expression of wolframin-antisense transcripts in BRIN-BD11 beta-cells. *Biochem. Biophys. Res. Commun.*, **307**, 684–688.
34. Sherr, C.J. and Roberts, J.M. (1999) CDK inhibitors: positive and negative regulators of G1-phase progression. *Genes Dev.*, **13**, 1501–1512.
35. Cozar-Castellano, I., Weinstock, M., Haughty, M., Velazquez-Garcia, S., Sipula, D. and Stewart, A.F. (2006) Evaluation of β-cell replication in mice transgenic for hepatocyte growth factor and placental lactogen. Comprehensive characterization of the G1/S regulatory proteins reveals unique involvement of $p21^{CIP1}$. *Diabetes*, **55**, 70–77.
36. Yang, L., Sara, G., Carlson, S.G., McBurney, D. and Horton, W.E., Jr (2005) Multiple signals induce endoplasmic reticulum stress in both primary and immortalized chondrocytes resulting in loss of differentiation, impaired cell growth, and apoptosis. *J. Biol. Chem.*, **280**, 31156–31165.
37. Zu, K., Bihani, T., Lin, A., Park, Y.M., Mori, K. and Ip, C. (2006) Enhanced selenium effect on growth arrest by BiP/GRP78 knockdown in p53-null human prostate cancer cells. *Oncogene*, **25**, 546–554.
38. Uchida, T., Nakamura, T., Hashimoto, N., Matsuda, T., Kotani, K., Sakaue, H., Kido, Y., Hayashi, Y., Nakayama, K.I., White, M.F. and Kasuga, M. (2005) Deletion of Cdkn1b ameliorates hyperglycemia by maintaining compensatory hyperinsulinemia in diabetic mice. *Nat. Med.*, **11**, 175–182.
39. Shi, Y., Taylor, S.I., Tan, S.L. and Sonenberg, N. (2003) When translation meets metabolism: multiple links to diabetes. *Endocr. Rev.*, **24**, 91–101.
40. Yoshida, H., Haze, K., Yanagi, H., Yura, T. and Mori, K. (1998) Identification of the *cis*-acting endoplasmic reticulum stress response element responsible for transcriptional induction of mammalian glucose-regulated proteins. *J. Biol. Chem.*, **273**, 33741–33749.
41. Lee, A.S. (2005) The ER chaperone and signaling regulator GRP78/Bip as a monitor of endoplasmic reticulum stress. *Methods*, **35**, 373–381.
42. Niwa, H., Yamamura, K. and Miyazaki, J. (1991) Efficient selection for high-expression transfectants with a novel eukaryotic vector. *Gene*, **108**, 193–199.
43. Tashiro, F., Niwa, H. and Miyazaki, J. (1999) Constructing adenoviral vectors by using the circular form of the adenoviral genome cloned in a cosmid and the Cre-loxP recombination system. *Hum. Gene Ther.*, **10**, 1845–1852.

# Cold Exposure Suppresses Serum Adiponectin Levels through Sympathetic Nerve Activation in Mice

*Junta Imai,*†‡¶ Hideki Katagiri,†‡¶ Tetsuya Yamada,*¶ Yasushi Ishigaki,* Takehide Ogihara,† Kenji Uno,*† Yutaka Hasegawa,*† Junhong Gao,*†‡ Hisamitsu Ishihara,* Hironobu Sasano,§ and Yoshitomo Oka**

**Abstract**

IMAI, JUNTA, HIDEKI KATAGIRI, TETSUYA YAMADA, YASUSHI ISHIGAKI, TAKEHIDE OGIHARA, KENJI UNO, YUTAKA HASEGAWA, JUNHONG GAO, HISAMITSU ISHIHARA, HIRONOBU SASANO, AND YOSHITOMO OKA. Cold exposure suppresses serum adiponectin levels through sympathetic nerve activation in mice. *Obesity.* 2006;14:1132–1141.

***Objective:*** Several lines of evidence suggest important roles for adiponectin in glucose and lipid metabolism and atherosclerosis. However, the mechanisms regulating serum adiponectin levels and adiponectin production are still not completely understood. Our aim was to determine whether adiponectin synthesis is physiologically regulated by the sympathetic nervous system (SNS).

***Research Methods and Procedures:*** Mice were exposed to cold (4 °C) for 12 hours and for 24 hours with or without inhibition of noradrenaline synthesis or pan-$\beta$ adrenergic function, followed by measurement of serum adiponectin concentrations and levels of adiponectin and uncoupling protein (UCP) 1 expressions in various white adipose tissues (WATs).

***Results:*** Cold exposure significantly reduced serum adiponectin concentrations without changing body weights or WAT sizes in either subcutaneous or intra-abdominal fat tissues. The serum adiponectin reduction was associated with a decrease in adiponectin mRNA expression in subcutaneous, epididymal, and mesenteric fat tissues. In these adipose tissues, UCP1 expression was markedly enhanced, suggesting SNS activation in these tissues. Administration of $\alpha$-methyl-*p*-tyrosine or a combination of SR59230A and propranolol reversed the cold-exposure–induced decreases in serum adiponectin concentrations and adiponectin mRNA expression in these tissues. In contrast, in retroperitoneal fat, the effects of cold exposure on adiponectin and UCP1 expressions were strikingly weak but were not reversed by SNS inhibitors.

***Discussion:*** SNS physiologically regulates serum adiponectin levels and adiponectin synthesis in WATs in vivo, although responsiveness to SNS stimulation differs markedly among WATs. Sympathetic activation might be involved in development of the metabolic syndrome by modulation of serum adiponectin concentrations.

**Key words: white adipose tissue, adipocytokine, $\alpha$-methyl-*p*-tyrosine, SR59230A, metabolic syndrome**

## Introduction

Obesity results from disruption of the balance between caloric intake and energy expenditure and is associated with insulin resistance (1). Insulin resistance is a fundamental contributor to the metabolic syndrome associated with type 2 diabetes, hypertension, hyperlipidemia, and atherosclerosis. Among the major advancements in this field were the discoveries of adipocyte-derived factors, such as leptin, adiponectin, free fatty acids (2), tumor necrosis factor-$\alpha$ (3), and plasminogen-activator inhibitor-1 (4). These adipocyte-derived factors play crucial roles in insulin sensitivity. Free fatty acids, tumor necrosis factor-$\alpha$, and plasminogen-activator inhibitor-1 reportedly contribute to development of insulin resistance in vivo and in vitro (2–4), whereas adiponectin increases insulin sensitivity.

Received for review April 8, 2005.
Accepted in final form April 5, 2006.
The costs of publication of this article were defrayed, in part, by the payment of page charges. This article must, therefore, be hereby marked "advertisement" in accordance with 18 U.S.C. Section 1734 solely to indicate this fact.
Divisions of *Molecular Metabolism and Diabetes and †Advanced Therapeutics for Metabolic Diseases, Center for Translational and Advanced Animal Research, ‡Tohoku University 21st Century COE Program "Comprehensive Research and Education Center for Planning of Drug Development and Clinical Evaluation," and §Department of Pathology, Tohoku University Graduate School of Medicine, Sendai, Japan.
¶ These authors contributed equally to the paper.
Address correspondence to Hideki Katagiri, Division of Advanced Therapeutics for Metabolic Diseases, Center for Translational and Advanced Animal Research, Tohoku University Graduate School of Medicine, 2-1 Seiryo-machi, Aoba-ku, Sendai 980-8575, Japan.
E-mail: katagiri@mail.tains.tohoku.ac.jp

Adiponectin was originally identified as a protein induced during adipogenesis (5–8). Low serum adiponectin levels were demonstrated in murine models of obesity and insulin resistance (6). In humans, serum adiponectin levels are inversely correlated with body weights and adiposity (9–11), suggesting important roles of adiponectin in the development of insulin resistance in obese subjects. In addition, adiponectin is reportedly involved in protection against atherosclerosis (12–14). Low serum levels of adiponectin are associated with atherogenesis in obese and insulin-resistant subjects (15,16). Therefore, to understand the pathophysiology of metabolic syndrome associated with insulin resistance and to develop novel therapeutic targets for the metabolic syndrome, it is essential to elucidate the mechanisms regulating adiponectin production and the resultant serum adiponectin levels.

There is considerable evidence that leptin is regulated by many types of stimuli (17–21). Notably, the sympathetic nervous system (SNS)[1] reportedly regulates leptin synthesis both in vitro and in vivo. In isolated brown and white adipocytes, leptin synthesis is suppressed by β3 adrenergic receptor (AR) agonists (18). In addition, SNS stimulation by acute cold exposure decreases leptin mRNA in white and brown adipose tissues (BATs) (22,23). Blockade of noradrenaline synthesis by α-methyl-*p*-tyrosine (α-MPT) causes marked increases in leptin mRNA in white adipose tissue (WAT) and plasma leptin levels (24). Thus, SNS activation suppresses leptin synthesis, thereby decreasing serum leptin in vivo.

In contrast, SNS involvement in adiponectin regulation is somewhat controversial. In 3T3-L1 adipocytes, isoproterenol, a β-adrenergic stimulant, reportedly reduced adiponectin mRNA, and this inhibitory effect was reversed by pretreatment with propranolol, a β-adrenergic antagonist (25). In mice, administration of a β-adrenergic stimulant reduced adiponectin mRNA expression in adipose tissue and serum adiponectin concentrations (26), suggesting SNS involvement in adiponectin regulation in vivo. However, Puerta et al. (22) reported that cold-exposure (18 hours at 6 °C)–induced SNS activation did not significantly affect adiponectin expression in WAT or the serum adiponectin concentrations in rats, although adiponectin mRNA levels were reduced in BAT. Conversely, cold exposure (24 hours at 4 °C) also reportedly increases serum adiponectin levels (27). Thus, the physiological role of SNS in adiponectin regulation is unclear and remains controversial. Therefore, to determine whether SNS is involved in physiological regulation of adiponectin synthesis in vivo, we exposed mice to cold environments with or without inhibition of noradrenaline synthesis or pan-β adrenergic function. To achieve inhibition of noradrenaline synthesis and β adrenergic function, mice were treated with α-MPT and a combination of SR59230A and propranolol, a β3 AR antagonist and a β1/β2 AR antagonist, respectively. We then examined the effects of these treatments on adiponectin expression in various WATs and on serum adiponectin concentrations. Herein, we report that, although the degrees of effects differed among WATs, cold exposure decreased adiponectin expression in subcutaneous, epididymal, and mesenteric fat tissues, resulting in significantly decreased serum adiponectin concentrations. Furthermore, the effects of cold exposure were suppressed by inhibition of noradrenaline synthesis or β adrenergic function. To our knowledge, this is the first study demonstrating that SNS activation physiologically influences serum adiponectin concentrations in vivo.

[1] Nonstandard abbreviations: SNS, sympathetic nervous system; AR, adrenergic receptor; BAT, brown adipose tissue; α-MPT, α-methyl-*p*-tyrosine; WAT, white adipose tissue; UCP, uncoupling protein; SE, standard error; PPAR, peroxisome proliferator activator.

## Research Methods and Procedures

### *Animals*

Animal studies were conducted under protocols in accordance with the institutional guidelines for animal experiments at Tohoku University. Ten-week-old male C57BL/6N mice were purchased from Clea (Tokyo, Japan), housed in an air-conditioned environment, with a 12-hour light-dark cycle, and fed a regular unrestricted diet. Mice were divided into two body-weight–matched groups; mice in the cold-stimulated group were placed in a cold room (4 °C) for 12 hours or for 24 hours with the same light-dark schedule as control mice, whereas for the control group, the temperature was 25 °C. In several experiments, 150 mg/kg body weight α-MPT (Sigma, St. Louis, MO) was intraperitoneally injected immediately before the exposure to 4 °C or 25 °C. In several other experiments, a combination of 1.5 mg/kg body weight SR59230A (Sigma) and 1.5 mg/kg body weight (*S*)-(−)-propranolol (Sigma) was intraperitoneally injected immediately before starting the experiment and then every 4 hours for the 24-hour duration of exposure to 4 °C or 25 °C. Body weights were measured before and after cold exposure. Food intake amounts during these periods were also determined. Blood samples were obtained before and immediately after cold exposure. The mice were then sacrificed and epididymal fat, subcutaneous fat, mesenteric fat, and retroperitoneal fat were rapidly removed, immediately frozen in liquid $N_2$, and stored at −80 °C until analysis.

### *Histological Analysis*

Each adipose tissue was stained with hematoxylin and eosin. Total adipocyte areas were traced manually and analyzed. Cell diameters were measured for 100 or more adipocytes in each group.

### *Immunoassay*

Serum adiponectin concentrations were measured using a mouse/rat adiponectin ELISA Kit (Otsuka Pharmacy, To-

kyo, Japan). The limit of sensitivity was 0.25 ng/mL, and the linearity limit was 8.0 ng/mL. Serum samples were diluted 1:10,000 with assay buffer before analysis.

### *Quantitative Reverse-Transcription-Polymerase Chain-Reaction-Based Gene Expression*

Total RNA was isolated from 100 mg of mouse WAT and 50 mg of BAT with ISOGEN (Wako Pure Chemical Co., Osaka, Japan), and cDNA synthesis was performed with a First Strand cDNA Synthesis Kit (Roche, Indianapolis, IN) using 1.0 μg of total RNA. cDNA synthesized from total RNA was evaluated in a real-time polymerase chain reaction quantitative system (Light Cycler Quick System 350S; Roche Diagnostics GmbH, Mannheim, Germany). The relative amount of mRNA was calculated with β-actin mRNA as the invariant control. The following oligonucleotide primers were used: adiponectin, CTGGAGAGAAGGGAGAGAAAGG (sense) and ACATTGGGAACAGTGACGCGGG (antisense); uncoupling protein (UCP) 1, TACCAAGCTGTGCGATGT (sense) and AAGCCCAATGATGTTCAGT (antisense); and β-actin, TTGTAACCAACTGGGACGATATGG (sense) and GATCTTGATCTTCATGGTGCTAGG (antisense).

### *Statistical Analysis*

The statistical significance of differences between groups was assessed by unpaired Student's *t* test. Data are presented as means ± standard error (SE).

## Results

### *Effects of Cold Exposure on Serum Adiponectin Concentration*

First, to determine the effects of cold exposure on adiponectin synthesis and serum adiponectin concentrations, mice were exposed to cold (4 °C). Twenty-four-hour cold exposure did not affect the fat content of WAT. For example, epididymal fat weight did not differ between the two groups (Table 1). In addition, histological analysis revealed that there were no significant differences in cell diameters of white adipocytes, including subcutaneous, epididymal, mesenteric, and retroperitoneal fat tissues, between control and cold-stimulated mice (Figure 1).

Although 24-hour cold exposure did not significantly affect cell sizes in WAT, where adiponectin is mainly produced, serum adiponectin concentrations were significantly decreased in response to 24-hour cold exposure (Figure 2A). We therefore examined the time course of alterations in serum adiponectin levels in response to cold stimulation, measuring adiponectin levels at 3, 6, 9, 12, and 24 hours of cold stimulation. Serum adiponectin levels decreased gradually throughout the experiment, and the difference in serum adiponectin levels between control mice and cold-stimulated mice reached statistical significance by 24 hours (Figure 2B). These data suggest that sympathetic nerve activation is involved in the regulation of serum adiponectin levels, irrespective of white adipocyte sizes.

Body weights of 12-hour cold-stimulated mice were significantly lower than those of control mice that had been exposed to 25 °C for 12 hours, whereas those of 24-hour cold-stimulated mice had been restored to the control level (Table 1). Food intake amounts of cold-stimulated mice were significantly higher than those of control mice (Table 1). These results suggest that cold stimulation accelerates energy expenditure and that hyperphagia after 12 hours restores body weight. Serum insulin and leptin levels were increased after 24- but not 12-hour cold exposure, whereas no significant changes were seen in lipid levels. In

**Table 1.** Parameters of 12-hr and 24-hr cold-stimulated mice

| | 12 hr | | 24 hr | |
|---|---|---|---|---|
| Parameter (units) | Room temperature (n = 6) | Cold stimulation (n = 7) | Room temperature (n = 6) | Cold stimulation (n = 8) |
| Total body weight (g) | 23.20 ± 0.18 | 21.38 ± 0.25* | 23.83 ± 0.28 | 24.00 ± 0.39 |
| Food intake (g) | ND | ND | 3.46 ± 0.17 | 7.20 ± 0.13* |
| Epididymal fat weight (mg) | ND | ND | 273.00 ± 11.9 | 268.67 ± 7.32 |
| TG (mg/dl) | 31.21 ± 5.21 | 25.19 ± 1.73 | 36.39 ± 2.88 | 38.31 ± 1.79 |
| T-Chol (mg/dl) | 86.88 ± 3.15 | 93.97 ± 2.11 | 82.72 ± 1.65 | 88.34 ± 1.19 |
| FFA (mEq/l) | 0.64 ± 0.10 | 0.72 ± 0.07 | 0.54 ± 0.029 | 0.21 ± 0.024* |
| Insulin (ng/ml) | 1.20 ± 0.16 | 1.39 ± 0.12 | 1.37 ± 0.16 | 3.35 ± 0.77† |
| Leptin (ng/ml) | 2.68 ± 0.18 | 2.22 ± 0.34 | 2.20 ± 0.40 | 4.33 ± 0.48† |
| Glucose (mg/dl) | 160.20 ± 5.16 | 167.00 ± 4.09 | 161.00 ± 2.24 | 167.40 ± 4.50 |

Data are presented graphically as means ± standard error of the mean.
* $p < 0.01$, † $p < 0.05$ vs. control as assessed by unpaired *t* test.

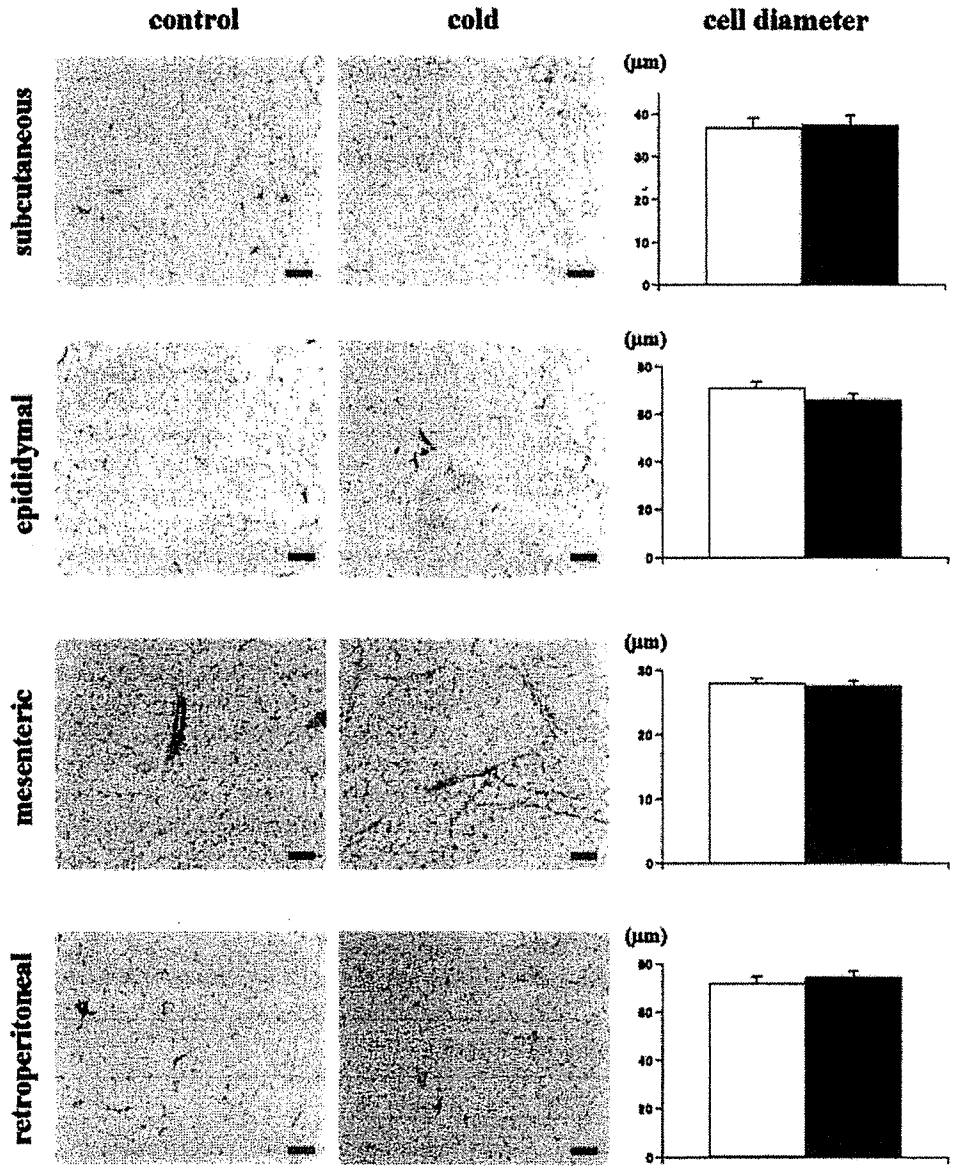


*Figure 1:* Effects of cold exposure on cell diameter in various WATs. Morphologies and cell diameters of adipocytes in subcutaneous, epididymal, mesenteric, and retroperitoneal fat tissues from control (white bars) and cold-stimulated (black bars) mice. Original magnification, ×100. Scale bar, 100 μm.

contrast, serum adiponectin levels were persistently decreased during cold stimulation (Figure 2B), suggesting it to be unlikely that these lipids and hormones have any major involvement in the adiponectin regulation observed in our experiments.

Next, to examine whether the serum adiponectin decrease induced by cold stimulation is due to decreased adiponectin production, we examined adiponectin mRNA expression levels in various WATs after 12- or 24-hour cold stimulation. Without cold stimulation, the adiponectin expression levels did not differ significantly among subcutaneous, mesenteric, epididymal, and retroperitoneal fat tissues (Figure 2C). Consistent with the results from the time course study of serum adiponectin levels, after 12-hour cold stimulation, adiponectin mRNA expressions in all adipose tissues examined tended to be decreased, but the differences did not reach statistical significance when compared with those in control mice. With 24-hour cold stimulation, de-

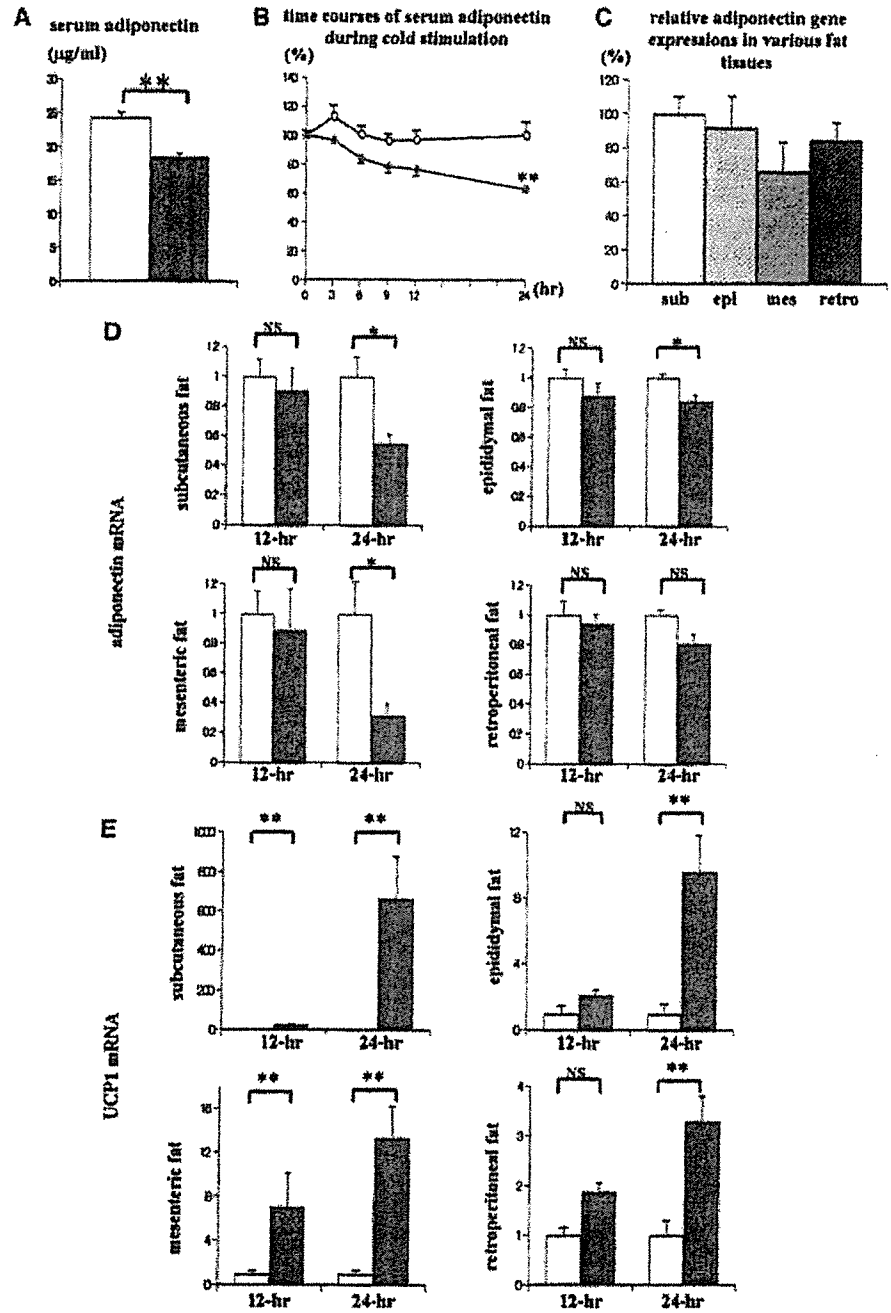


*Figure 2:* Effects of cold exposure on serum adiponectin concentrations, adiponectin, and UCP1 mRNA expressions in various WATs. (A) Serum adiponectin concentrations of control (open bars) and 24-hour cold-stimulated mice (gray bars) (control mice exposed to 25 °C, cold-stimulated mice to 4 °C). (B) Time courses of serum adiponectin in control (open circles) and cold-stimulated (filled circles) mice. *y*-Axis indicates percentage changes from baseline. (C) Relative adiponectin gene expressions in subcutaneous (sub), epididymal (epi), mesenteric (mes), and retroperitoneal (retro) fat. *y*-Axis indicates percent expressions of subcutaneous fat tissue. In each fat tissue, the relative amounts of adiponectin mRNA were calculated with β-actin mRNA as the invariant control. Data are presented graphically as means ± SE ($n$ = 15 per each fat tissue). (D) Adiponectin mRNA expression levels in various WATs of control (open bars) and cold-stimulated (gray bars) mice after a 12- or 24-hour exposure to cold. (E) UCP1 mRNA expression levels in various fat tissues of control (open bars) and cold-stimulated (gray bars) mice after a 12-or 24-hour exposure to cold. Data are presented graphically as means ± SE ($n$ = 6 per group). * $p < 0.05$ and ** $p < 0.01$ vs. control as assessed by unpaired Student's $t$ test.

clines in adiponectin mRNA expressions in subcutaneous, epididymal, and mesenteric fat tissues became significant, whereas those in retroperitoneal fat tissue did not (Figure 2D). Thus, cold stimulation decreased adiponectin expression in various fat tissues, resulting in a decrease in serum adiponectin, although the effects of cold stimulation on adiponectin synthesis seem to differ markedly among various WATs. Taken together with the report that the number of cells in subcutaneous fat is ~75% of that in all adipose tissue of lean mice (28), adiponectin expression in subcutaneous fat is likely to contribute greatly to its serum concentration.

SNS activation reportedly increases UCP1 expression in WAT (29,30). Therefore, to investigate the degrees of activation of sympathetic nerves by various fat tissues in response to cold stimulation, we next examined UCP1 mRNA expressions in various WATs. In control mice (at 25 °C), the levels of UCP1 mRNA did not differ significantly among WATs, including subcutaneous, epididymal, mesenteric, and retroperitoneal fat (data not shown). In subcutaneous fat tissue, cold stimulation markedly increased UCP1 mRNA expression levels, 29- and 664-fold with 12- and 24-hour cold stimulation, respectively. With 12-hour cold stimulation, modest increases in UCP1 expression were observed in epididymal and mesenteric fat tissues, 2- and 7-fold; with 24-hour cold stimulation, there were further increases of 10- and 13-fold, respectively. On the other hand, the magnitude of the increment in UCP1 expression in retroperitoneal fat tissue was much smaller than those in other WATs (Figure 2E). Thus, cold stimulation activated sympathetic nerves to WATs, but the degree of the effects of cold stimulation, such as UCP1 induction, differed among WATs.

### *Effects of SNS Inhibitors on Serum Adiponectin Concentration after Cold Exposure*

Next, to examine directly whether the serum adiponectin concentration decrease is due to SNS activation, mice were treated with α-MPT, a specific inhibitor of tyrosine hydroxylase, the rate-limiting enzyme in the synthesis of noradrenaline (31). In a previous study, to completely inhibit the SNS activation, mice were administered α-MPT intraperitoneally at a dose of 300 mg/kg body weight (24). In our preliminary study, therefore, we also administered 300 mg/kg body weight α-MPT. At this dose, however, all of the mice died during cold exposure, presumably due to diminished heat production resulting from complete blockage of SNS activation. Therefore, we administered 150 mg/kg body weight α-MPT. At this dose, ~70% of mice survived the full duration of cold exposure. We examined serum adiponectin concentrations and adiponectin expression levels in WAT using the mice that had survived throughout cold exposure. It is noteworthy that the inhibitory effects of α-MPT on SNS activation were partial, not complete.

With α-MPT administration, cold stimulation had no effect on body weights. The increment in food intake with cold stimulation was also observed in α-MPT-administered mice. Similarly, cold exposure had no impact on WAT weights (data not shown).

Serum adiponectin concentrations tended to be decreased in response to cold exposure with α-MPT administration, but the decreases were not statistically significant (Figure 3A). The magnitude of cold-exposure–induced decrements in serum adiponectin levels was significantly blunted by α-MPT administration (Figure 3B). Thus, partial inhibition of SNS activation reversed the serum adiponectin reduction, which clearly indicates involvement of SNS in regulating serum adiponectin levels. To further elucidate the mechanisms whereby SNS activation affects serum adiponectin concentrations, alterations in adiponectin mRNA levels in response to cold stimulation were examined in WAT with and without α-MPT administration. Administration of α-MPT reversed the cold-stimulation–induced decreases in adiponectin expression in subcutaneous, epididymal, and mesenteric fat tissues (Figure 3C). In retroperitoneal fat tissue, however, α-MPT administration had no effect on adiponectin expression (Figure 3C). These findings suggest that cold stimulation decreases adiponectin expression in various WATs by SNS activation, resulting in decreased serum adiponectin levels, although the degrees of the responses to cold stimulation differ markedly among WATs.

To confirm the diverse effects of SNS activation on various WATs, alterations in UCP1 mRNA levels in response to cold stimulation were examined in WAT with and without α-MPT administration. In subcutaneous fat tissue, although cold stimulation markedly enhanced UCP1 expression, this enhancement was inhibited with α-MPT administration (664- vs. 34-fold) (Figure 3D). In epididymal and mesenteric fat tissues, α-MPT administration clearly reversed the increase in UCP1 expression induced by cold stimulation (Figure 3D). In contrast, in retroperitoneal fat tissue, α-MPT administration did not significantly suppress UCP1 expression (Figure 3D). These findings indicated SNS involvement in the regulation of adiponectin expression in adipose tissues and the resultant serum adiponectin concentration, although the effects of cold stimulation were relatively small in retroperitoneal fat tissue.

Next, to determine whether β adrenergic function is involved in adiponectin regulation, mice were simultaneously administered 1.5 mg/kg body weight SR59230A, a β3 AR antagonist, and 1.5 mg/kg body weight (*S*)-(−)-propranolol, a β1/β2 AR antagonist. In a previous study, to inhibit sympathetic stimulation, these inhibitors were administered at the same doses that we used, and the effects were ana-

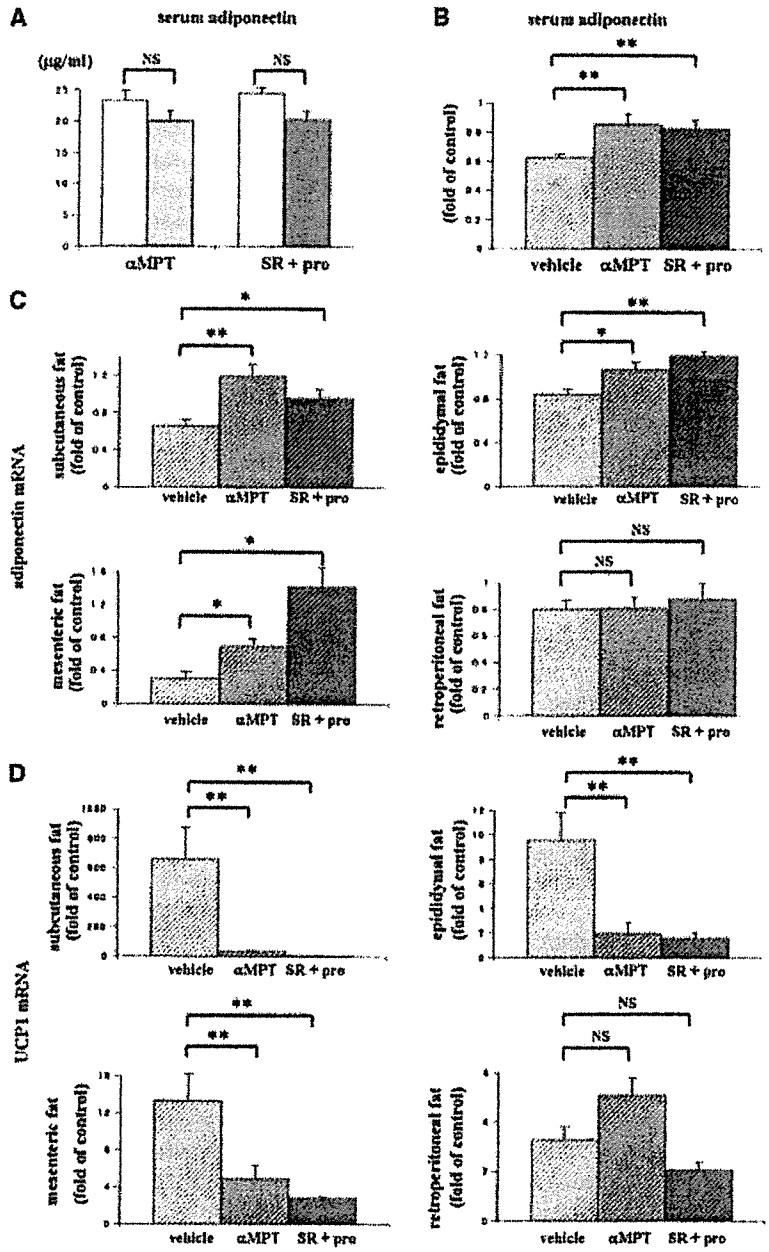


*Figure 3:* Effects of cold exposure with SNS inhibitor administration on serum adiponectin concentrations and adiponectin and UCP1 mRNA expressions in various WATs. (A) Serum adiponectin concentrations of control (open bar) and cold-stimulated mice given α-MPT (light gray bar) or a combination of SR59230A and propranolol (dark gray bar). Data are presented graphically as means ± SE (α-MPT-control; $n = 6$, α-MPT-cold stimulated; $n = 10$, SR + pro-control; $n = 4$, SR + pro-cold stimulated; $n = 5$). * $p < 0.05$ and ** $p < 0.01$ vs. control as assessed by unpaired Student's $t$ test. (B) Magnitudes of serum adiponectin concentration change after cold exposure (vehicle) and those with α-MPT (α-MPT) or a combination of SR59230A and propranolol (SR + pro) administration. (C) Magnitudes of adiponectin mRNA expression changes after cold exposure (vehicle) and those with α-MPT (α-MPT) or a combination of SR59230A and propranolol (SR + pro) administration. (D) Magnitudes of UCP1 mRNA expression change after cold exposure (vehicle) and those given α-MPT (α-MPT) or a combination of SR59230A and propranolol (SR + pro). (B to D) Each parameter of 24-hour cold-stimulated mice was divided by the mean level in room-temperature-conditioned mice given the same treatment. Data are presented graphically as means ± SE (α-MPT-control, $n = 6$; α-MPT-cold-stimulated, $n = 10$; SR + pro-control, $n = 4$; SR + pro-cold-stimulated, $n = 5$). * $p < 0.05$ and ** $p < 0.01$ vs. cold exposure with vehicle.

lyzed 4 hours after administrations (32). Therefore, we administered these drugs to control and cold-stimulated mice every 4 hours for 24 hours. In our experiment, all mice survived after 24-hour cold exposure. The results were very similar to those obtained with α-MPT administration. Suppression of increased UCP1 expression in subcutaneous, epididymal, and mesenteric fat tissues confirmed effective blockade of β3 adrenergic function in these adipose tissues (Figure 3D). Adrenergic blockade inhibited the effects of cold stimulation on adiponectin expression in these fat tissues (Figure 3C) and serum adiponectin concentrations (Figure 3, A and B). In retroperitoneal fat tissue, administration of these β AR inhibitors did not significantly affect cold-exposure–induced alterations in the expression of adiponectin (Figure 3C) or UCP1 (Figure 3D). Our findings clearly show that the aforementioned adiponectin regulation by SNS is mediated mainly by β ARs. In addition, in retroperitoneal fat tissue, there appears to be little, if any, SNS involvement in metabolic activities.

## Discussion

Several lines of evidence have recently suggested that adiponectin is involved in glucose and lipid metabolism. In mice, systemic adiponectin treatment increased fatty acid oxidation in muscle (33), decreased plasma glucose by enhancing the ability of insulin to suppress hepatic glucose production (34), and improved insulin sensitivity in insulin-resistant models (35). In addition, loss of the adiponectin gene in mice reportedly decreased insulin responsiveness and enhanced atherogenesis (16,36). Furthermore, a central action of adiponectin was reported: a decrease in body weight due to stimulation of energy expenditure (37). Together, these data strongly suggest that adiponectin plays an important role in preventing development of the metabolic syndrome.

Despite the physiological significance of adiponectin, the mechanism regulating serum adiponectin is still not completely understood. In the present study, cold exposure, which activates SNS physiologically, reduced adiponectin expression in various WATs, resulting in a significant decrease in the serum adiponectin concentration. In addition, administration of a noradrenaline synthesis inhibitor or β AR inhibitors inhibited cold-exposure–induced reductions in serum adiponectin levels and adiponectin expression in WATs. These findings clearly show that SNS activation, especially β stimulation, is involved in regulating the production of adiponectin and its serum levels. There is considerable evidence that adiponectin correlates negatively with body weight (9–11). In addition, adiponectin expression is reportedly decreased in enlarged adipocytes (38). However, in the present study, it is noteworthy that body weights and adipocyte sizes did not differ, regardless of 24-hour cold exposure and/or SNS inhibitor administration. These findings indicate that, independently of alterations in adiposity, SNS regulates adiponectin production and the resultant serum adiponectin levels.

Peroxisome proliferator activator (PPAR) γ reportedly increases adiponectin expression in WAT (39). However, in this study, no significant alterations were observed in PPARγ mRNA expression in various WATs of mice subjected to cold stimulation (data not shown), suggesting that cold-stimulated alteration of adiponectin mRNA expression in WAT is not mediated by increased PPARγ expression.

In contrast to our study, Puerta et al. (22) reported that, in rats, acute cold exposure did not significantly change adiponectin expression in WAT or the serum adiponectin concentration. The reasons for this discrepancy are not known, but differences in the magnitude and periods of cold exposure might explain the differing results. In our study, mice were exposed to 4 °C for 24 hours, whereas in the previous report, rats were subjected to milder cold stimulation, i.e., 6 °C for 18 hours. Alternatively, mice might be more sensitive to cold stimulation than rats. In any case, in the present study, administering a noradrenaline synthesis inhibitor or β AR inhibitors reversed the effects of cold stimulation, confirming involvement of SNS, especially β adrenergic function, in the regulation of adiponectin synthesis in WAT. Because it is well known that SNS is activated in obese subjects (40,41), decreased serum adiponectin levels in obese subjects might be, at least partly, attributable to SNS hyperactivity.

Another interesting finding in this study is the markedly different degrees of responsiveness to cold exposure among WATs. In response to cold stimulation, in subcutaneous fat tissue, UCP1 expression was increased 664-fold. In contrast, in retroperitoneal fat tissue, the increase was only 3- to 4-fold, although without cold stimulation, the UCP1 mRNA levels did not differ significantly among these WATs. In addition, although SNS inhibitor administration reversed the increases in UCP1 expression in subcutaneous, epididymal, and mesenteric fat tissues, such inhibitors did not affect UCP1 expression in retroperitoneal fat tissue. Furthermore, in contrast to other fat tissues studied, the decrease in adiponectin expression after cold exposure was not significant in retroperitoneal fat tissue. Thus, the metabolic alteration induced by SNS activation differs markedly among various fat tissues and is especially small in retroperitoneal fat tissue.

The differences in responsiveness among various WATs might be explained by how abundant the nerve supply to these fat tissues is. Alternatively, sympathetic nerves to retroperitoneal fat might not be fully activated by cold stimulation. Differential activations of SNS innervating different tissues, in response to various stimuli, have reportedly been observed. For instance, in contrast to cold stimulation, intracerebroventricular injection of 2-deoxyglucose, which activates many sympathetic nerves, suppresses the activation of sympathetic nerves to BAT (42). In addition, it

was recently reported that hypothalamic phosphoinositide 3-kinase and mitogen-activated protein kinase differentially regulate different regional sympathetic activations in response to intracerebroventricular injection of insulin (43). In the present study, we recognized that responsiveness to cold stimulation differs mechanistically among various WATs according to anatomical location. Although further studies are necessary for elucidating the mechanisms in detail, the different responses to SNS stimulation might be involved in the diverse characteristics of adipocytes according to anatomical location. Increased adiposity in various fat tissues contributes in different ways to the development of the metabolic syndrome (44,45), which might, at least in part, be explained by the magnitude of activation of sympathetic nerves to each fat tissue.

## Acknowledgments

We thank I. Sato, K. Kawamura and M. Hoshi for technical support. This work was supported by a Grant-in-Aid for Scientific Research (B2, 15390282 to H.K.) and by a Grant-in-Aid for Exploratory Research (15659214 to H.K.) from the Ministry of Education, Science, Sports, and Culture of Japan and by a Grant-in-Aid for Scientific Research (H16 genome-003 to Y.O.) from the Ministry of Health, Labor, and Welfare of Japan. This work was also supported by the 21st Century COE Program Special Research Grant "the Center for Innovative Therapeutic Development for Common Diseases" from the Ministry of Education Science, Sports, and Culture (to Y.O.).

### References

1. **Kahn BB, Flier JS.** Obesity and insulin resistance. *J Clin Invest.* 2000;106:473–81.
2. **Bluher M, Kratzsch J, Paschke R.** Plasma levels of tumor necrosis factor-alpha, angiotensin II, growth hormone, and IGF-I are not elevated in insulin-resistant obese individuals with impaired glucose tolerance. *Diabetes Care.* 2001;24: 328–34.
3. **Hotamisligil GS.** The role of TNFalpha and TNF receptors in obesity and insulin resistance. *J Intern Med.* 1999;245:621–5.
4. **Shimomura I, Funahashi T, Takahashi M, et al.** Enhanced expression of PAI-1 in visceral fat: possible contributor to vascular disease in obesity. *Nat Med.* 1996;2:800–3.
5. **Scherer PE, Williams S, Fogliano M, Baldini G, Lodish HF.** A novel serum protein similar to C1q, produced exclusively in adipocytes. *J Biol Chem.* 1995;270:26746–9.
6. **Hu E, Liang P, Spiegelman BM.** AdipoQ is a novel adipose-specific gene dysregulated in obesity. *J Biol Chem.* 1996;271: 10697–703.
7. **Maeda K, Okubo K, Shimomura I, Funahashi T, Matsuzawa Y, Matsubara K.** cDNA cloning and expression of a novel adipose specific collagen-like factor, apM1 (AdiPose Most abundant Gene transcript 1). *Biochem Biophys Res Commun.* 1996;221:286–9.
8. **Nakano Y, Tobe T, Choi-Miura NH, Mazda T, Tomita M.** Isolation and characterization of GBP28, a novel gelatin-binding protein purified from human plasma. *J Biochem (Tokyo).* 1996;120:803–12.
9. **Arita Y, Kihara S, Ouchi N, et al.** Paradoxical decrease of an adipose-specific protein, adiponectin, in obesity. *Biochem Biophys Res Commun.* 1999;257:79–83.
10. **Yang WS, Lee WJ, Funahashi T, et al.** Weight reduction increases plasma levels of an adipose-derived anti-inflammatory protein, adiponectin. *J Clin Endocrinol Metab.* 2001;86: 3815–9.
11. **Weyer C, Funahashi T, Tanaka S, et al.** Hypoadiponectinemia in obesity and type 2 diabetes: close association with insulin resistance and hyperinsulinemia. *J Clin Endocrinol Metab.* 2001;86:1930–5.
12. **Okamoto Y, Kihara S, Ouchi N, et al.** Adiponectin reduces atherosclerosis in apolipoprotein E-deficient mice. *Circulation.* 2002;106:2767–70.
13. **Ouchi N, Kihara S, Arita Y, et al.** Adipocyte-derived plasma protein, adiponectin, suppresses lipid accumulation and class A scavenger receptor expression in human monocyte-derived macrophages. *Circulation.* 2001;103:1057–63.
14. **Yamauchi T, Kamon J, Waki H, et al.** Globular adiponectin protected ob/ob mice from diabetes and ApoE-deficient mice from atherosclerosis. *J Biol Chem.* 2003;278:2461–8.
15. **Hotta K, Funahashi T, Arita Y, et al.** Plasma concentrations of a novel, adipose-specific protein, adiponectin, in type 2 diabetic patients. *Arterioscler Thromb Vasc Biol.* 2000;20: 1595–9.
16. **Kubota N, Terauchi Y, Yamauchi T, et al.** Disruption of adiponectin causes insulin resistance and neointimal formation. *J Biol Chem.* 2002;277:25863–6.
17. **Li H, Matheny M, Tumer N, Scarpace PJ.** Aging and fasting regulation of leptin and hypothalamic neuropeptide Y gene expression. *Am J Physiol.* 1998;275:E405–11.
18. **Gettys TW, Harkness PJ, Watson PM.** The beta 3-adrenergic receptor inhibits insulin-stimulated leptin secretion from isolated rat adipocytes. *Endocrinology.* 1996;137:4054–7.
19. **Kumar MV, Scarpace PJ.** Differential effects of retinoic acid on uncoupling protein-1 and leptin gene expression. *J Endocrinol.* 1998;157:237–43.
20. **Bradley RL, Cheatham B.** Regulation of ob gene expression and leptin secretion by insulin and dexamethasone in rat adipocytes. *Diabetes.* 1999;48:272–8.
21. **Havel PJ.** Role of adipose tissue in body-weight regulation: mechanisms regulating leptin production and energy balance. *Proc Nutr Soc.* 2000;59:359–71.
22. **Puerta M, Abelenda M, Rocha M, Trayhurn P.** Effect of acute cold exposure on the expression of the adiponectin, resistin and leptin genes in rat white and brown adipose tissues. *Horm Metab Res.* 2002;34:629–34.
23. **Trayhurn P, Duncan JS, Rayner DV.** Acute cold-induced suppression of ob (obese) gene expression in white adipose tissue of mice: mediation by the sympathetic system. *Biochem J.* 1995;311:729–33.
24. **Rayner DV, Simon E, Duncan JS, Trayhurn P.** Hyperleptinaemia in mice induced by administration of the tyrosine hydroxylase inhibitor alpha-methyl-*p*-tyrosine. *FEBS Lett.* 1998;429:395–8.

25. **Fasshauer M, Klein J, Neumann S, Eszlinger M, Paschke R.** Adiponectin gene expression is inhibited by beta-adrenergic stimulation via protein kinase A in 3T3-L1 adipocytes. *FEBS Lett.* 2001;507:142–6.
26. **Delporte ML, Funahashi T, Takahashi M, Matsuzawa Y, Brichard SM.** Pre- and post-translational negative effect of beta-adrenoceptor agonists on adiponectin secretion: in vitro and in vivo studies. *Biochem J.* 2002;367:677–85.
27. **Yoda M, Nakano Y, Tobe T, Shioda S, Choi-Miura NH, Tomita M.** Characterization of mouse GBP28 and its induction by exposure to cold. *Int J Obes Relat Metab Disord.* 2001;25:75–83.
28. **Trayhurn P, James WP, Gurr MI.** Studies on the body composition, fat distribution and fat cell size and number of "Ad," a new obese mutant mouse. *Br J Nutr.* 1979;41:211–21.
29. **Bouillaud F, Ricquier D, Mory G, Thibault J.** Increased level of mRNA for the uncoupling protein in brown adipose tissue of rats during thermogenesis induced by cold exposure or norepinephrine infusion. *J Biol Chem.* 1984;259:11583–6.
30. **Nagase I, Yoshida T, Kumamoto K, et al.** Expression of uncoupling protein in skeletal muscle and white fat of obese mice treated with thermogenic beta 3-adrenergic agonist. *J Clin Invest.* 1996;97:2898–904.
31. **Moore KE, Dominic JA.** Tyrosine hydroxylase inhibitors. *Fed Proc.* 1971;30:859–70.
32. **Evans BA, Agar L, Summers RJ.** The role of the sympathetic nervous system in the regulation of leptin synthesis in C57BL/6 mice. *FEBS Lett.* 1999;444:149–54.
33. **Fruebis J, Tsao TS, Javorschi S, et al.** Proteolytic cleavage product of 30-kDa adipocyte complement-related protein increases fatty acid oxidation in muscle and causes weight loss in mice. *Proc Natl Acad Sci USA.* 2001;98:2005–10.
34. **Berg AH, Combs TP, Du X, Brownlee M, Scherer PE.** The adipocyte-secreted protein Acrp30 enhances hepatic insulin action. *Nat Med.* 2001;7:947–53.
35. **Yamauchi T, Kamon J, Waki H, et al.** The fat-derivedhormone adiponectin reverses insulin resistance associated with both lipoatrophy and obesity. *Nat Med.* 2001;7:941–6.
36. **Maeda N, Shimomura I, Kishida K, et al.** Diet-induced insulin resistance in mice lacking adiponectin/ACRP30. *Nat Med.* 2002;8:731–7.
37. **Qi Y, Takahashi N, Hileman SM, et al.** Adiponectin acts in the brain to decrease body weight. *Nat Med.* 2004;10:524–9.
38. **Yang X, Jansson PA, Nagaev I, et al.** Evidence of impaired adipogenesis in insulin resistance. *Biochem Biophys Res Commun.* 2004;317:1045–51.
39. **Iwaki M, Matsuda M, Maeda N, et al.** Induction of adiponectin, a fat-derived antidiabetic and antiatherogenic factor, by nuclear receptors. *Diabetes.* 2003;52:1655–63.
40. **Scherrer U, Randin D, Tappy L, Vollenweider P, Jequier E, Nicod P.** Body fat and sympathetic nerve activity in healthy subjects. *Circulation.* 1994;89:2634–40.
41. **Alvarez GE, Beske SD, Ballard TP, Davy KP.** Sympathetic neural activation in visceral obesity. *Circulation.* 2002;106:2533–6.
42. **Egawa M, Yoshimatsu H, Bray GA.** Effects of 2-deoxy-D-glucose on sympathetic nerve activity to interscapular brown adipose tissue. *Am J Physiol.* 1989;257:R1377–85.
43. **Rahmouni K, Morgan DA, Morgan GM, et al.** Hypothalamic PI3K and MAPK differentially mediate regional sympathetic activation to insulin. *J Clin Invest.* 2004;114:652–8.
44. **Pouliot MC, Despres JP, Nadeau A, et al.** Visceral obesity in men: associations with glucose tolerance, plasma insulin, and lipoprotein levels. *Diabetes.* 1992;41:826–34.
45. **Abate N, Garg A, Peshock RM, Stray-Gundersen J, Grundy SM.** Relationships of generalized and regional adiposity to insulin sensitivity in men. *J Clin Invest.* 1995;96:88–98.